



# Simulating secondary organic aerosol from anthropogenic and biogenic precursors: comparison to outdoor chamber experiments, effect of oligomerization on SOA formation and reactive uptake of aldehydes

Florian Couvidat<sup>1</sup>, Marta G. Vivanco<sup>2</sup>, and Bertrand Bessagnet<sup>1</sup>

<sup>1</sup>Institut National de l'Environnement Industriel et des Risques, Verneuil-en-Halatte, France

<sup>2</sup>Centro de Investigaciones Energéticas, Medioambientales y Tecnológicas (CIEMAT), Departamento de Medio Ambiente, Av. Complutense 40, 28040-Madrid, Spain

Correspondence to: Florian Couvidat  
([Florian.Couvidat@ineris.fr](mailto:Florian.Couvidat@ineris.fr))

## Abstract.

New parameterizations for the formation of organic aerosols have been developed. These parameterizations cover SOA formation from biogenic and anthropogenic precursors, NO<sub>x</sub> dependency, oligomerization and the reactive uptake of pinonaldehyde. Those parameterizations are based on available experimental results.

5 The effects of those parameterizations are tested against various experiments carried out in previous studies inside the outdoor chamber Euphore. Two datasets of experiments were used : the anthropogenic experiments (where SOA is formed mainly from a mixture of toluene, 1,3,5-trimethylbenzene and o-xylene) and the biogenic experiments (where SOA is formed mainly from  $\alpha$ -pinene and limonene). SOA formation inside the chamber is simulated by using the Secondary Organic Aerosol Processor (SOAP) model to take into account the dynamic evolution of concentrations.

10 When assuming no wall deposition of organic vapors, satisfactory results were obtained for the biogenic experiments and most of the anthropogenic experiments. However, the anthropogenic experiments seem to indicate a complex NO<sub>x</sub> dependency that could not be reproduced by the model. Oligomerization was found to have a strong effect on SOA composition and could have a strong effect on the formation of SOA. The uptake of pinonaldehyde (which is a high volatility SVOC) onto acidic aerosol was found to be too slow to occur under atmospheric conditions but less volatile or more reactive aldehydes could react  
15 in acidic aerosols indicating that the parameterization of Pun and Seigneur (2007) used in some air quality models may lead to an overestimation of SOA concentrations.

However, taking into account wall deposition of organic vapors (with the parameters of Zhang et al. (2014)) leads to a strong underestimation of SOA concentrations. This feature is consistent with the fact that the SOA mechanisms are based on environmental chamber data. This underestimation could however be corrected by decreasing the volatility of SVOC by a factor 3.

20 The effect of particle viscosity was also estimated. A low effect of viscosity on SOA concentrations was simulated by the model. However, taking it into account leads to a decrease of SVOC evaporation and prevents changes in concentration due to changes of temperature during the experiments.



## 1 Introduction

Because of the effect of fine particles on human health (WHO, 2003) and ecosystems (Kanakidou et al., 2005), it is necessary to develop models able to predict particle formation in order to evaluate its impact and to evaluate mitigation strategies. As particulate organic matter (OM) represents a large fraction of the total fine particulate mass, typically between 20 and 60% (Kanakidou et al., 2005; Yu et al., 2007; Zhang et al., 2007), efforts have to be made to represent OM as accurately as possible in models. Secondary Organic Aerosols (SOA) represent most of OM (90% according to the best estimate of Kanakidou et al. (2005)).

Numerous models have been developed to simulate OM in 3D air quality models (Schell et al., 2001; Donahue et al., 2006, 2011; Pun et al., 2002; Couvidat et al., 2012; Griffin et al., 2003; Jathar et al., 2015; Tulet et al., 2006; Carlton et al., 2010; Menut et al., 2013). Most models use simple parameterizations based on yields estimated from smog chamber experiments conducted under specific conditions, which can be different from atmospheric conditions (low humidity, specific NO<sub>x</sub> conditions) based on chamber experiment results even if several studies (Zhang et al., 2014, 2015; Bian et al., 2015) showed that gas wall deposition of organic vapors could lead to a strong underestimation of SOA yields. Moreover, SOA parameterizations need to take into account the effects of NO<sub>x</sub> concentrations or oligomerization as those effects have been shown to greatly affect the level of SOA predicted by models (e.g. Ng et al. (2007a, b); Pun and Seigneur (2007); Couvidat and Seigneur (2011); Hall IV and Johnston (2011)). Therefore, it is necessary to develop parameterizations gathering all these phenomena.

Moreover, none of these models take into account all the complexity of the processes involved in organic aerosol formation (non-ideality, multi-phase partitioning, viscosity of the aerosol, phase separation, aging, oligomerization and organosulfate formation, etc...). Some of these processes were treated in the Secondary Organic Aerosol Processor (SOAP) (Couvidat and Sartelet, 2015), a 0D model that can be used to take into account non-ideality, multi-phase partitioning, phase separation and the viscous state of OM.

Oligomer formation has been addressed in some modeling studies. This process may be important for organic aerosol as it can transform semi-volatile and volatile organic compounds into less volatile compounds. Trump and Donahue (2014) studied the effect of oligomerization on the dynamic of organic aerosol formation. Pun and Seigneur (2007) developed a parameterization for the oligomerization of aldehydes by increasing the partitioning coefficient of aldehydes. This parameterization (treating oligomerization with an equilibrium constant) have been used in Couvidat et al. (2012) to increase the partitioning of pinonaldehyde. High aerosol concentrations were simulated with this parameterization. However, Liggio and Li (2006b) showed that the uptake of pinonaldehyde onto acidic aerosol is a slow process and that this process could be due to oligomerization but also to organosulfate formation. Carlton et al. (2010) used a simple first-order rate constant of oligomerization for all organic compounds based on the results of Kalberer et al. (2004). Lemaire et al. (2015) compared all these approaches and emphasized the need to simulate properly oligomerization in air quality models.

In this study, several parameterizations are developed and the results of the model are tested against SOA formation (from biogenic and anthropogenic precursors) experiments performed in the outdoor chamber Euphore. The parameterizations developed concern the oxidation mechanisms of biogenic ( $\alpha$ -pinene, limonene) and anthropogenic (toluene, trimethylbenzene)



precursors, oligomerization and the dynamic uptake of pinonaldehyde onto acidic aerosols.

The goal of this study is to evaluate how several processes and parameterizations could affect SOA modeling. In a first part, a new SOA mechanism developed with a common methodology based on SOA yields (methodology of Odum et al. (1996)) is tested under conditions different from the conditions under which it was developed (mixture of different compounds, non-controlled temperature). In a second part, the effect of particle phase reactions is investigated. For that purpose, a parameterization for oligomerization was developed to evaluate the impact of oligomerization and the results given by the equilibrium based parameterization of Pun and Seigneur (2007) is compared to the results given by a dynamic parameterization based on the results of Liggio and Li (2006b) for the uptake of pinonaldehyde onto acidic aerosol. The results of these two parameterizations are compared to results from SOA formation experiments in the presence of SO<sub>2</sub> (that lead to the formation of an acidic aerosol). Finally, the effects of low diffusion inside the particle due to high viscosity and of wall losses of organic vapors are studied.

## 2 Method

New parameterizations described hereafter are developed and tested against experiments that were previously carried out inside the outdoor chamber Euphore in Valencia.

### 2.1 Experimental datasets

The experiments used for the comparison between the model and experiments have been published in previous studies (Vivanco et al., 2011, 2013). The Euphore facility is described in Volkamer et al. (2001). Although the experimental dataset was designed for model evaluation purposes, it was not designed to evaluate the model developed in this study. Vivanco et al. (2016) and Santiago et al. (2012) used these experiments to evaluate simple parameterizations existing in several air quality models. The experiments may not cover all ranges of values covered by the model for some parameters, especially for relative humidity (RH) which was lower than 40% for all experiments.

Two datasets of experiments are used: (i) the anthropogenic experiments where SOA is formed from the oxidation of toluene, 1,3,5-trimethylbenzene and to a lesser extent o-xylene and octane and (ii) the biogenic experiments where SOA is formed from  $\alpha$ -pinene and limonene and to a lesser extent isoprene. Experimental conditions for the anthropogenic and biogenic experiments are described respectively in Tables 1 and 2. For the biogenic dataset, two experiments were carried out in presence of SO<sub>2</sub> to evaluate the parameterization of Pun and Seigneur (2007). Due to its low SOA yield, SOA from isoprene oxidation should not represent a significant amount of total SOA.

Although octane is a precursor of SOA and is present in the anthropogenic experiments, SOA formation from octane oxidation was not taken into account in this study as Vivanco et al. (2016) showed with an experiment in the same chamber that octane lead to an insignificant amount of SOA. Due to its low yield (0.5% according to Lim and Ziemann (2005)), octane SOA should not represent more than a few percent of total SOA.



PM volume concentrations were measured with a Scanning Mobility Particle Sizer Spectrometer (SMPS).

## 2.2 Model development

Secondary organic aerosols inside the chamber were simulated by coupling the gas-phase mechanism RACM2 (Goliff et al., 2013) with the SOAP model (Couvidat and Sartelet, 2015) to compute the dynamic formation of SOA. RACM2 was used because it has been shown to perform well for oxidant formation (Kim et al., 2009). To represent the chemical evolution of SVOC, RACM2 was modified to take into account the formation of the surrogate species according to the mechanisms described hereafter. The ROS2 algorithm (Verwer et al., 1999) was used to solve the chemical kinetic equations.

SOAP is a model designed to be modular with user options depending on the computation time. SOAP uses the surrogate approach to estimate several properties and parameters (hygroscopicity, absorption into the aqueous phase of particles, activity coefficients and phase separation) and to evaluate the partitioning of organic compounds between one or several organic phases (the number of organic phases is determined by Gibbs energy minimization) and the inorganic phase. It accounts for the influence of interactions between organic and inorganic compounds by using the AIOMFAC algorithm (Zuend et al., 2008, 2011; Zuend and Seinfeld, 2012). Secondary inorganic aerosol formation was added to the SOAP model by using the equilibrium parameters of ISORROPIA v2.1 (Fountoukis and Nenes, 2007).

Currently, SOAP assumes that inorganic aerosols are metastable liquids and therefore does not take into account efflorescence or deliquescence processes. This assumption could be wrong in presence of ammonia due to the low humidity inside the chamber, as ammonium sulfate would probably be solid as humidity in the chamber (below 40%) is always far below the deliquescence relative humidity (80% at 298K). However, no ammonia was present for any experiments and SO<sub>2</sub> was only introduced for two experiments. For those two experiments, SO<sub>2</sub> oxidation will lead to sulfuric acid formation which remains liquid over the full RH range (Seinfeld and Pandis, 1998).

Several experimental data were used to constrain the model. Temperature and relative humidity measurements inside the chamber were used as inputs for the model. SMPS measurements were used to compute the mean diameter of particles. The diameter of particle was used to compute the kinetic rate of condensation/evaporation/diffusion and the Kelvin effect by the dynamic approach of SOAP. The mean diameter of particles was constrained to provide the model with a realistic estimation of the diameter without modeling the nucleation in SOAP.

The model results were compared to non-corrected (according to wall losses) results. Wall deposition of particles was simulated via first order loss rate parameter constrained to reproduce the loss of particles during the last hours of the experiment when the chamber was closed.

Wall losses of vapors were not taken into account due to the lack of information on deposition onto Euphore walls. However, in the last section, the effect of vapor wall losses on SOA formation in the chamber was investigated by taking into account vapor wall losses according to parameters estimated (Zhang et al., 2014) for the Caltech chamber.



### 2.2.1 SOA Mechanism

A new mechanism was developed for SOA formation from toluene (TOL), xylene (XYL) and trimethylbenzene (TMB). Parameters were fitted based on data issued from various studies under low and high  $\text{NO}_x$  conditions: Ng et al. (2007b) for Toluene SOA, Ng et al. (2007b); Cocker III et al. (2001) for Xylene SOA and Cocker III et al. (2001) for TMB SOA. No information was found on SOA formation from TMB oxidation under low- $\text{NO}_x$  conditions, therefore, the stoichiometric coefficient from the low- $\text{NO}_x$  conditions for xylene was used. Similarly to Vivanco et al. (2016), the low- $\text{NO}_x$  condition yield are used only if radicals formed from the oxidation of the precursors react at least twice with the  $\text{HO}_2$  radical, to prevent high formation of low- $\text{NO}_x$  SOA under intermediate  $\text{NO}_x$  conditions. Molecular structures used by SOAP to estimate several properties and to compute activity coefficients were selected based on the results of Im et al. (2014) by selecting the compound with a similar volatility, formed in the largest quantity and ensuring the best reproduction of the O/C and H/C ratios. Reactions and properties of surrogate species are shown in Tables 3 and 7.

For monoterpenes, the mechanism of Pun et al. (2006) was updated using results from more recent studies. For SOA formation from  $\alpha$ -pinene,  $\beta$ -pinene and limonene ozonolysis, the mechanism is based on the parameterizations described in Lee et al. (2011) for high and low  $\text{NO}_x$  conditions. The API + OH reaction is based on the results of Svendby et al. (2008) whereas for the LIM + OH, the yield of BiA2D was optimized to give the better results. Reactions and properties of surrogate species are shown in Tables 3 and 7.

The terpene +  $\text{NO}_3$  yields are based on Fry et al. (2014).

In the surrogate SOA approach, results of the model may depend on the choice of the surrogate structure to represent SOA formation. Although different VOCs form different compounds (or the same compounds in different quantities), this approach lumps together species that have similar properties (like saturation vapor pressure) and are expected to have similar chemical structure. For example, first-generation aldehyde products from terpene oxidation were represented by the surrogate species BiA0D. Moreover, the compounds were selected (based on the best information available on SOA products) to reproduce the mean properties of SOA and of the O/C and H/C ratios. Kim et al. (2014) showed that the mean O/C and H/C ratios are around 0.34-0.36 and 1.4-1.5 for SOA from  $\alpha$ -pinene and limonene respectively. The selected surrogates give a O/C between 0.3 and 0.44 and a H/C between 1.55 and 1.6. For TOL SOA, the chosen surrogates give a O/C ratio (between 0.71 and 0.8) and H/C ratio (between 1.14 and 1.6) similar to the reported values by Schilling (2015) (between 0.7 and 0.8 for O/C and between 1.2 and 1.6 for H/C). For TMB SOA, Sato et al. (2012) indicate a O/C ratio around 0.4-0.6 and a H/C around 1.5-1.7. The chosen surrogates reproduce the O/C ratio (between 0.38 and 0.55) but seem to underestimate the high H/C ratio (between 1.13 and 1.44 due to the low H/C of the AnIP2 compound). However, for AnIP2, a better molecular structure having a similar O/C ratio and saturation vapor pressure could not be found.

The mechanism of Couvidat and Seigneur (2011) was used to simulate SOA formation from isoprene.



### 2.2.2 Oligomerization

Carlton et al. (2010) developed a parameterization for oligomerization based on a simple first-order rate constant of oligomerization. Based on the results of Kalberer et al. (2004) indicating 50% of polymers after 20h in TMB SOA, Carlton et al. (2010) determined a kinetic constant of  $9.6 \times 10^{-6} \text{ s}^{-1}$ . However, this number was obtained with a laser desorption ionization–mass spectrometry (LDI-MS) by taking all compounds with  $m/z$  higher than 400 (with  $m$  the ion mass and  $z$  the ion charge) and may not take into account small oligomers (dimers or trimers that may be formed more rapidly). Kalberer et al. (2004) and Kalberer et al. (2006) also studied the oligomer fraction based on a volatility tandem differential mobility analyzer (VTDMA) giving the remaining volume fraction of particles at different temperatures. They found that for TMB SOA, the remaining fraction at  $100^\circ\text{C}$  after 5h ranges from 50% to 62% and is composed of small oligomers or very low volatility organic compounds. The remaining fraction at  $100^\circ\text{C}$  can even reach and 80% to 90% after 25h. Based on this results and assuming that the remaining fraction is mainly composed of small oligomers and that oligomerization is irreversible, the first-order constant of oligomerization should be around  $3.85 \times 10^{-5} \text{ s}^{-1}$  to take into account small oligomer formation.

However, Roldin et al. (2014) showed that oligomerization should involve second order reversible reactions like esterification, hemiacetalization, aldolization, peroxyhemiacetalization. The equilibrium of these reactions are unfavored by humid conditions and the reaction is catalyzed under acidic conditions. Indeed, oligomer formation by esterification was reported in the case of isoprene SOA (Surratt et al., 2006). In this study, oligomerization is represented like a reversible process which is mainly due to mechanisms like esterification, unfavored by humid conditions. Oligomers are represented by simple species to know if “monomer blocks” are present mainly as oligomers or as monomers. If a monomer block from a compound reacts with another monomer block (from the same compound or from another compound), the compound will be converted from monomer to oligomer. The parameterization currently does not take into account different kinetic rate parameters between each combination of compounds due to lack of data. It assumes that a compound A reacting with itself will have the same kinetic parameter than a compound B reacting with itself and will have the same value when compounds A and B react together.

Oligomerization is represented by a simple “reduced” reaction:



with  $A$  a monomer compound,  $A_{oligo}$  the monomer blocks of compound A inside oligomers,  $m_{oligo}$  the number of monomer blocks inside oligomers,  $k_{oligo}$  the kinetic rate parameter of oligomerization and  $k_{reverse}$  the kinetic rate parameter of the reverse reaction. If more data are available, the parameterization could be improved to take into account different kinetic rate parameters of oligomerization per combination.

The net flux of oligomerization  $J_{oligo}$  is computed using activities instead of concentrations for two main reasons. First, chemical rates are more consistent with thermodynamic equilibrium by computing rates using activities. Second, some studies (Madon and Iglesia, 2000; Rahimpour, 2004) express the need to compute chemical rates using activities and show that it gives better results for non-ideal systems.

$$J_{oligo} = -\frac{dX_{a,monomer}}{dt} = k_{oligo}a_{a,monomer} - k_{reverse}a_{a,oligomer} \quad (2)$$



with  $X_{a,monomer}$  the molar fraction of compound,  $a_{a,monomer}$  activity on a molar fraction basis of compound a and  $a_{a,oligomer}$  activity on a molar fraction basis of the oligomer formed from compound a.

The kinetic rate of oligomerization  $k_{oligo}$  is computed as follows:

$$k_{oligo} = k_{oligo}^{max} a_{monomer} \quad (3)$$

- 5 with  $k_{oligo}^{max}$  the maximum kinetic rate parameter for oligomerization, and  $a_{monomer}$  the sum of monomer activities.

To calculate the reverse kinetic rate parameter, the computation is based on the equilibrium oligomerization constant  $K_{oligo}^{eq}$ . The equilibrium constant for oligomerization (due to esterification or a similar oligomerization mechanism) is computed with:

$$K_{oligo}^{eq} = \frac{a_{a,oligomer} a_{H_2O}^{m_{oligo}-1}}{a_{a,monomer}^{m_{oligo}-1}} \quad (4)$$

- 10 At equilibrium, the rate of oligomerization is zero. Therefore,

$$\frac{k_{oligo}^{max}}{k_{reverse}} = \frac{a_{a,oligomer}/m_{oligo}}{a_{monomer} a_{a,monomer}} = \frac{(K_{oligo}^{eq})^{m_{oligo}-1} a_{monomer}^{m_{oligo}-2}}{a_{H_2O}^{m_{oligo}-1}} \quad (5)$$

- To represent oligomerization,  $k_{oligo}^{max}$ ,  $m_{oligo}$  and  $K_{oligo}^{eq}$  were estimated based on the results of Kalberer et al. (2006). In this study, the molar masses of heavy molecules in SOA from several precursors were measured using matrix-assisted laser desorption/ionization mass spectrometry (MALDI-MS). To do that, we represented explicitly the formation of oligomers up to tetramers from a single monomer using the kinetic rate parameter and the equilibrium constant for oligomerization to simulate the evolution of mass averaged molar mass of oligomers (which cannot be simulated with our reduced parameterization for oligomerization because the molar mass of oligomers does not vary with this parameterization). The equilibrium constant of oligomerization  $K_{oligo}^{eq}$  and the oligomerization constant  $k_{oligo}^{max,extended}$  of the extended parameterization were fitted so that the evolution as a function of time of the weight average molar mass of oligomers during the first hours of the experiment is reproduced by the model as shown by Fig. 2. A molar mass of the TMB SOA monomer of 155 g/mol was chosen so that the molar mass of TMB SOA is between 140 and 170 g/mol based on Im et al. (2014).  $m_{oligo}$  and  $k_{oligo}^{max}$  are chosen so that the molar averaged mean molar mass and the total mass of oligomers (with oligomers and monomers) of the reduced and the extended parameterizations are similar. The reduced parameterization values found for  $k_{oligo}^{max}$ ,  $m_{oligo}$  and  $K_{oligo}^{eq}$  were respectively  $2.2 \times 10^{-4} \text{ s}^{-1}$ , 3.35 and 2.94 for TMB SOA.  $k_{oligo}^{max}$  is in the same order of magnitude as the kinetic rate parameter reported for the reaction acetaldehyde and methanol by Roldin et al. (2014):  $4.9 \times 10^6 \text{ a}[\text{H}^+] \text{ M h}^{-1}$  ( $\text{a}[\text{H}^+]$  being the activity of  $\text{H}^+$ ), which should be around  $6 \times 10^{-4} \text{ s}^{-1}$  on an activity basis for a pH of 4.6 (order of magnitude of pKa for carboxylic acids).

- This reduced parameterization only takes into account the formation of short oligomers but should give a good insight on the impact of oligomerization on SOA formation. Formation of short oligomers can impact SOA formation by transforming monomers and increasing the condensation of semi-volatile compounds onto the particle. However, big oligomers formation should affect less SOA formation as it should mainly lead to the transformation of oligomers into bigger oligomers. Big oligomers could affect indirectly the partitioning of monomers by increasing the mean molar mass of the organic phase; the



partitioning constant of monomers being inversely proportional to the mean molar mass.

This parameterization also gives good results for the isoprene SOA oligomerization using a molar mass of 120 g/mol. This molar mass corresponds to the molar mass of methyl glyceric acid, which was shown to undergo oligomerization by esterification. For  $\alpha$ -pinene, Kalberer et al. (2006) did not find any significant temporal evolution of oligomer molar masses, which is consistent with a dimer formation that cannot react further and therefore parameters for oligomerization of  $\alpha$ -pinene SOA cannot be evaluated.

The results for SOA oligomerization from TMB and isoprene for the extended and reduced parameterizations are shown in Fig. 2. For the formation of dimers from  $\alpha$ -pinene, we used the same parameters except for  $m_{oligo}$  is set to 2 to limit the formation of oligomers to dimers. DePalma et al. (2013) confirmed that particle-phase dimer formation is possible. However Kristensen et al. (2014) studied the formation of 4 dimers and determine that for those 4 dimers are not formed from particle-phase reaction through gas-phase reactions of the stabilized Criegee Intermediate formed from the ozonolysis of  $\alpha$ -pinene. It could then be possible that in the case of  $\alpha$ -pinene not all the oligomers are formed via particle-phase reactions.

In this study, the second order parameterization was used for simulations. In case of the oligomerization inside an aqueous acidic phase, a kinetic rate of  $8.76 a[H^+]$  should be used to take into account the effect of acidity on oligomerization.

### 2.2.3 Uptake of pinonaldehyde onto acidic aerosols

Several studies (Liggio and Li, 2006a, b) reported an uptake of pinonaldehyde onto acidic aerosols higher than what could be predicted by assuming equilibrium between the gas and particle phases and no chemical reaction inside the particles. This phenomenon is attributed to oligomer and/or organosulfate formation. Gao et al. (2004b) reported a similar phenomenon for various aldehydes. To represent this phenomenon, Pun and Seigneur (2007) developed a parameterization by computing an effective Henry's law constant  $H_{eff}$  for aldehyde compounds:

$$H_{eff} = H \left( 1 + 0.1 \left( \frac{a(H^+)}{10^{-6}} \right)^{1.91} \right) \quad (6)$$

where  $H$  is the monomer Henry's law constant of the compound, and  $a(H^+)$  is the activity of protons in the aqueous phase. As fine particles are generally very acidic (Ludwig and Klemm, 1990; Keene et al., 2004), uptake of pinonaldehyde will in fact appear to be an irreversible process, even though the parameterization is formulated as a reversible process. Using this parameterization for pinonaldehyde in 3D air quality models leads to very high concentrations of SOA from monoterpenes (Couvidat et al., 2012).

However, this parameterization does not take into account the uptake kinetic rate of aldehydes. Liggio and Li (2006b) measured the uptake rate coefficients for various acidities of the aerosols. The authors showed that the uptake of pinonaldehyde onto aerosols can only be significant for very high acidities (which can be reached with low ammonia concentration and at low humidities). Based on these results, a parameterization for the chemical evolution of pinonaldehyde has been developed in this study:







with  $\text{BiA0D}_{part}$  the amount of pinonaldehyde inside the particle and  $k_{trans}$  (in  $\text{s}^{-1}$ ), the kinetic rate of BiA0D transformation inside the particle into a product assumed non-volatile. Liggio and Li (2006b) did not evaluate a kinetic rate of pinonaldehyde transformation inside the particle but a kinetic of uptake. However, the kinetic of uptake can be linked to the kinetic of transformation by assuming equilibrium between the gas and particle phases:

$$5 \quad k_{uptake} = k_{trans} K_{aq} A Q \quad (8)$$

with  $K_{aq}$  the partition coefficient of pinonaldehyde between the gas phase and the particle and  $AQ$  the particle mass.

As in Liggio and Li (2006b), the pH of particles and activities of compounds were computed with AIOMFAC (Zuend et al., 2008, 2011; Zuend and Seinfeld, 2012; Ganbavale et al., 2015) according to experimental conditions. The estimated flux of transformation based on the results of Liggio and Li (2006b) was plotted against several variables to find the variables exhibiting the best correlations.  $m_{H^+}$  the molality of ion  $H^+$  and  $a_{HSO_4^-}^{(m)}$  the activity as a molality basis of ion  $HSO_4^-$  were found to be the best variables with high correlation coefficients (0.98 for  $m_{H^+}$  and 0.92 for  $a_{HSO_4^-}^{(m)}$ ) with the chemical flux of transformation pinonaldehyde  $J_{trans}$  inside the particle. Fig. 1 shows  $J_{trans}$  (in  $\text{s}^{-1}$ ) as a function of  $m_{H^+}$  (in mol/kg) and  $a_{HSO_4^-}^{(m)}$  (in mol/kg).

Two possible parameterizations can therefore be used to take into account the possible transformation of pinonaldehyde in the particle phase: the  $H^+$ -dependent parameterization and the  $HSO_4^-$ -dependent parameterization. For the  $H^+$ -dependent parameterization, the kinetic rate is computed as:

$$k_{trans} = 2.01 \times 10^{-7} \times \exp(0.297 m_{H^+}) \quad (9)$$

whereas the  $HSO_4^-$ -dependent parameterization is computed with:

$$k_{trans} = 1.53 \times 10^{-7} a_{HSO_4^-}^{(m)} \quad (10)$$

In that case, we assume that the reaction leads to the formation of the organosulfate formed from pinonaldehyde.

The  $H^+$ -dependent parameterization could be representative of an oligomerization mechanism catalyzed by  $H^+$  ion. However, in that case, the uptake of pinonaldehyde should be seen as a reversible pathway which also depends on the humidity of the experiments. The  $HSO_4^-$ -dependent parameterization could be representative of organosulfate formation and therefore pinonaldehyde should in that case act as a sink for sulfates due to the reaction between sulfates and pinonaldehyde.

### 2.3 Aging mechanism

To test the influence of aging on SOA formation, an aging mechanism was developed. The aging of BiA0D is based on the results of Chacon-Madrid and Donahue (2013) who studied SOA formation from pinonaldehyde oxidation. SOA formation from BiA1D is based on the SOA yield from the oxidation of pinonic acid as measured by Müller et al. (2012). For the aging of BiA2D, the parameterizations of Jathar et al. (2015) were used to determine the amount of functionalization and the decrease of volatility due to aging. Nopinone, which is formed from the oxidation of  $\beta$ -pinene was shown to form a significant amount



of SOA and low-volatility products (Sato et al., 2016). Nopinone was included in the mechanism. SOA yields from nopinone oxidation was based on Mutzel et al. (2016). The yields of formation of nopinone were based on Hakola et al. (1994) for the reaction of  $\beta$ -pinene with OH and O<sub>3</sub> and on Hallquist et al. (1999) for the reaction of  $\beta$ -pinene with NO<sub>3</sub>. Kinetics for aging were taken from the Master Chemical Mechanism v3.3.1 (Jenkin et al., 1997; Saunders et al., 2003).

5 For the aging of aromatic SOA compounds, the parameterizations of Jathar et al. (2015) were used to determine the amount of functionalization and the decrease of volatility due to aging. According to this study, oxidation of aromatics should mainly lead to the addition of one oxygen atom. For simplification purposes, we assumed that aging of aromatic SOA leads to the addition a single hydroxy group.

Table 6 shows the aging mechanism used in this study.

10 This simple mechanism was developed in order to be able to assess the capacity to form oligomers and of the reactive uptake of pinonaldehyde in the long-term formation of SOA.

## 2.4 Long-term SOA formation simulations

The experimental conditions (low relative humidity, oxidation over a few hours, high organic mass loading) are probably very different from typical ambient conditions. To evaluate more precisely the potential effect of oligomerization, SOA formation  
15 over 3 days of evolution with an organic mass loading of 5  $\mu\text{g m}^{-3}$  from the oxidation of  $\alpha$ -pinene, toluene and TMB was simulated for various humidities with or without oligomerization. The simulated effect of oligomerization is compared to the simulated effect of aging on SOA formation. Octane and NO<sub>x</sub> concentrations are set in order to reproduce a level of OH concentrations similar to summer conditions (around 0.001 ppb during daytime). The diurnal cycle was simulated by computing the evolution of the zenith angle at Valencia as a function of local time. This diurnal profile was simulated to take into account  
20 that oxidation and aging slow down during night (due to the low concentrations of radicals) whereas oligomerization continues. On the other hand, the relative humidity was assumed constant (whereas under ambient conditions relative humidity probably has a diurnal profile) and the structures of pinonic acid for simulations with  $\alpha$ -pinene and of AnRP2 for simulations with toluene and TMB oxidation are used for the structure of the organic loading. Those simulations are not representative of atmospheric conditions but can be used to illustrate the effect of long-term oligomerization on SOA formation. For simulations  
25 with oligomerization, the fraction of monomers inside the aerosol is assumed to be one, i.e., the aerosol is assumed to be mainly constituted by monomers that can react with absorbed compounds. These simulations provide therefore information on the maximal effect that oligomerization can have on SOA yields.

## 3 Results

The simulated degradation of precursors is illustrated in Figures S1 and S2 in supplementary materials. Whereas the mechanism was able to reproduce the degradation of VOC during the beginning of the experiments, medium-term oxidation of toluene  
30 seems to be underestimated for some experiments (A1, A3, A4 and A7). Due to this, medium-term formation of toluene SOA



may be underestimated.

### 3.1 Comparison with measurements

Figures 3 and 5 show the results of the model for the biogenic experiments without SO<sub>2</sub> and the anthropogenic experiments respectively. Simulated SOA composition for simulations considering oligomerization are illustrated in Supplementary Materials in Figures S3 (biogenic experiments) and S4 (anthropogenic experiments). In these simulations, the wall deposition rate was constrained to reproduce the loss of particles during the last hours of the experiment when the chamber was closed as described in section 2.2. Therefore, the wall deposition rate used with and without oligomerization are different. To examine the effect of the wall deposition rate, the formation of SOA with oligomerization was also simulated with the deposition rate as computed by the simulation without oligomerization.

For the biogenic experiments, the model gives good results with or without oligomerization for all experiments with slightly better results without oligomerization for experiment B5 and slightly better results with oligomerization for experiment B1. The experiments B2, B3, B4 and B5 have previously been modeled by Santiago et al. (2012) using a box model version of two air quality models: CMAQ (Carlton et al., 2010) and Chimere (Menuet et al., 2013). The authors found a significant overestimation of modeled SOA which was not found with the model used in this study.

For the anthropogenic experiments, the model gives satisfactory results (with or without oligomerization) for experiment A1, A3, A6 and A7 but overestimates concentrations by 30-40% for A2 and A5 and underestimates concentrations by 25% for A8 and A9.

Concentrations for experiment A4 are overestimated by a factor 2. However, experimental conditions for experiment A4 are close to those of experiment A1, except for HONO concentrations which are two times higher than for experiment A4. The model gives similar results for A1 (for which the model gives satisfactory results) and A4. It could not explain why concentrations were so different between these two experiments. One possibility is that anthropogenic SOA formation is inhibited at high HONO concentrations.

The alternation of overestimation and underestimation events could be related to differences in chemical regimes. To compare the chemical regimes of the experiments, a ratio representative of the chemical regime (called hereafter “chemical regime ratio”) was computed with the sum of VOC concentrations multiplied by their reactivity with OH divided by NO<sub>x</sub> concentrations:

$$C_r = \frac{\sum_i k_{OH,i} C_i}{C_{NO_x}} \times 10^{10} \quad (11)$$

with  $C_r$  the chemical regime ratio,  $C_i$  the concentration in ppb of each VOC and  $C_{NO_x}$  the concentration in ppb of NO<sub>x</sub>,  $k_{OH,i}$  the reactivity with OH in molecule<sup>-1</sup> cm<sup>3</sup> s<sup>-1</sup>. 10<sup>10</sup> is a factor set so that the values are close to unity.

It appears that experiments with a low chemical regime ratio (experiments A8 and A9 which have ratios of 0.13 and 0.7 respectively) underestimate SOA concentrations, whereas experiments that overestimate concentrations (experiments A2 and A5) have a high chemical regime ratio (the ratios are equal to 2.2 and 1.64). Other experiments (except A4) have a chemical



regime ratio between 0.77 and 1.05 and give satisfactory results. It may indicate a more complex  $\text{NO}_x$  dependency than what is represented in the model.

### 3.2 Effect of oligomerization on SOA formation

According to the model, the biogenic and anthropogenic experiments show a low effect of the oligomerization on SOA mass in the chamber as shown by Figures 3 and 5. Concentrations are indeed similar with and without oligomerization with low differences compared to the amount of SOA. Although the amount of SOA does not significantly change, the composition of SOA is strongly affected by oligomerization. Indeed, the oligomer content (in mass) at the end of the experiment varies from 68% to 78% for the biogenic experiments and from 38% to 58% for the anthropogenic experiments with a similar range of humidity (between 0.4% and 37%). For a 55% relative humidity, Gao et al. (2004a) determined for  $\alpha$ -pinene that the oligomer content of SOA could be well over 50%. This result is consistent with the results of our parameterization as an oligomer content around 60% was simulated for such an humidity.

The results of long-term SOA formation simulations are shown in Figures 6, 7 and 8. Without taking into account aging, oligomerization leads to a significant increase of concentrations after 3 days of evolution even at high humidity. Increase factors due to oligomerization are 2.5 for  $\alpha$ -pinene, 2.0 for toluene and 6.2 for TMB for a relative humidity of 30% and are 1.8 for  $\alpha$ -pinene, 1.4 for toluene and 3.3 for TMB for a relative humidity of 70%. Oligomerization is therefore a process that could significantly affect long term SOA formation.

Assuming aging leads to a slight decrease of SOA mass due to fractionalization for toluene SOA or an increase of concentrations due to functionalization for TMB and  $\alpha$ -pinene SOA. However, the effect of aging on SOA formation simulated here seems less important than the effect of oligomerization.

The different parameterizations of oligomerization are also compared in Fig. 6: the equilibrium second order reaction parameterization developed in this study, the first order complete reaction of Carlton et al. (2010) with a kinetic rate parameter of  $9.6 \times 10^{-6} \text{ s}^{-1}$  (halftime of 20h) and a kinetic rate parameter of  $3.85 \times 10^{-5} \text{ s}^{-1}$  (halftime of 5h). The three different parameterizations have different impact on SOA formation. The first order parameterization with a kinetic rate parameter of  $9.6 \times 10^{-6} \text{ s}^{-1}$  has a low impact on SOA yield except after a few days of oligomerization. With the kinetic rate parameter of  $3.85 \times 10^{-5} \text{ s}^{-1}$ , the increase of SOA yield can be significant after 10 hours, for RH=70% the SOA yield increases by 72% after one day. The second order parameterization gives a faster SOA production. However, this figure shows the maximal effect of the second-order parameterization (molar fraction of oligomers of 1). Depending on conditions, the second order parameterization could only have a low impact on SOA concentrations and the formation of oligomers could rapidly reach an equilibrium.

Depending on the conditions, oligomerization could also lead to a decrease of SOA concentrations as the partitioning is inversely proportional to the mean molar mass of organic aerosols (Pankow, 1994), which will increase with the oligomer formation. Increasing the mean molar mass by a factor 2 leads to a decrease around 40% of the SOA formed without oligomerization, indicating that the partitioning of monomers are sensitive to the value of the mean molar mass.



### 3.3 Uptake of pinonaldehyde onto acidic aerosols

The pH and  $\text{HSO}_4^-$  parameterizations and the parameterization of Pun and Seigneur (2007) assuming equilibrium are compared and evaluated against experiments B6 and B7 where  $\alpha$ -pinene and limonene are oxidized in the presence of  $\text{SO}_2$ . The oxidation of  $\text{SO}_2$  leads to the formation of sulfuric acid and therefore to acidic aerosols. The amount of SOA formed with each parameterization is compared to the results of the experiments (Fig. 4).

The parameterization of Pun and Seigneur (2007) leads to a significant overestimation of SOA concentrations. With this parameterization, BiAOD is entirely absorbed by the acidic aerosol. On the contrary, using the pH and  $\text{HSO}_4^-$  parameterizations which take into account the dynamic of the uptake, no significant formation of SOA is formed by this pathway. The two parameterizations give almost the same results than assuming no uptake.

Pinonaldehyde was found to be too volatile to form significant SOA by this pathway. The long-term formation of SOA by this pathway is tested with the simulation described in the previous section but in the presence of  $2 \mu\text{g}/\text{m}^3$  of sulfuric acid. Fig. 6 shows that even at low humidity ( $\text{RH}=30\%$ ), the amount of SOA formed is not significant after 3 days of evolution. Therefore, SOA formation from the reactive uptake by acidic acid of pinonaldehyde probably does not contribute significantly to SOA formation.

However, it could be possible that aldehyde compounds less volatile than pinonaldehyde react and form significant amount of SOA by this pathway. To test this hypothesis, we assumed that organosulfate could be formed from the compounds AnRP1 and AnRP2 (which have an aldehyde group in their molecular surrogate structure) using the  $\text{HSO}_4^-$  parameterization. The kinetic rate parameter should be specific of the compound but the  $\text{HSO}_4^-$  parameterization probably provides a good estimate and order of magnitude. Fig. 9 shows the amount of organosulfate that would be formed by this pathway for a humidity of 70% from the oxidation of toluene. Long-term organosulfate formation seems possible by this pathway (even at high humidity) as significant amount of organosulfate (13 to 18% of SOA) is formed with this assumption and that a significant mass of aldehydes has been converted into organosulfates. However, if high concentrations of ammonia are present in the atmosphere, pH will increase and  $\text{HSO}_4^-$  will decrease. In case of high concentrations of ammonia, the kinetic rate could be too low for this process to be significant.

this process would need for sulfate to not be fully neutralized by ammonia.

### 3.4 Investigation of the effect of particle-phase diffusion and wall losses of organic vapors

To evaluate the effect of the particle phase viscosity on SOA formation, the SOAP model was run for a particle-phase coefficient diffusion of  $2 \times 10^{-16} \text{ molecules}/\text{cm}^2/\text{s}$  which correspond to the order of magnitude of values determined for toluene SOA at low humidities (Song et al., 2016). To investigate wall losses of organic vapors, a first-order wall loss rate coefficient for vapors of  $2.5 \times 10^{-4} \text{ s}^{-1}$  was used as in Zhang et al. (2014) (value determined for the Teflon chamber of Caltech). Effect of the particle-phase viscosity and wall losses of vapor is illustrated in Fig. 10 for experiment A7. Results for other experiments (biogenic and anthropogenic) are similar to this experiment and are illustrated in Supplementary Materials in figures S5 and



S6.

Generally, similar results are obtained between non-viscous and viscous aerosols. Assuming viscous aerosols can lead to an increase of SOA concentrations due to the limitation of evaporation with low diffusion. As found by Couvidat and Sartelet (2015), condensation of low volatility compounds is possible without diffusing into the particle by condensing at the gas/particle interface. The condensation of low volatility compounds can create a layer onto which more volatile compounds can condense to respect Raoult's law at the interface. However, viscosity can prevent the evaporation of those more volatile compounds by preventing their diffusion from the core of the particle to the interface. For non-viscous aerosols, deposition of particles to wall can lead to the evaporation of SVOC due to a decrease of the absorbing mass.

Assuming viscous aerosols can also lead to a decrease of SOA sensitivity to change of conditions during the experiments. For example, experiment A5 is characterized by a decrease of the temperature during the experiment that lead to a decrease of volatility. Whereas concentrations increase when assuming non-viscous aerosols, concentrations seem unaffected by the change of temperature when assuming viscous aerosols (as compounds are absorbed by the core of particles with a slow kinetic rate). The shape of modeled SOA concentration curve is closer to measurement when assuming viscous aerosols.

Taking into account wall losses of vapors leads to a strong decrease of SOA concentrations, particularly for the anthropogenic experiments (decrease up to a factor 3) due to the lower organic aerosol loading compared to the biogenic experiments. The fact that the model underestimates SOA formation when assuming that vapors can condense onto the wall chamber is not surprising as the developed mechanism is based on the methodology of Odum et al. (1996) by using experimental results from Teflon chambers. As stronger organic aerosol loading favors condensation onto organic aerosol over condensation onto walls, wall losses of vapor may produce a shift in apparent volatilities; the organic aerosol formed in chambers may appear more volatile than it should be. For both the biogenic and anthropogenic experiments, results can be corrected by decreasing the saturation vapor pressures by a factor 3 as better or similar results could be obtained than without taking into account wall losses of organic vapors. These results indicate that volatility determined by the use of Odum's curves could be overestimated by a significant factor. However, wall deposition of organic vapors could also lead to an underestimation of stoichiometric coefficients.

25

#### 4 Conclusions

Several parameterizations were developed in this study. First, the chemical mechanism of Couvidat et al. (2012) was updated. The performance of the new mechanism was evaluated by comparison to experimental results from previous studies carried out in the Euphore chamber in Valencia. Second, parameterizations to take into account oligomerization and the uptake of pinonaldehyde onto acidic aerosols were developed. Finally, the effects of particle viscosity and wall deposition of vapors were investigated.

Without taking into account wall losses of vapors, good performances are obtained for the biogenic experiments. However, the experiments used for the comparison have high organic aerosol loading (between 50 and 150  $\mu\text{g}/\text{m}^3$ ) whereas low aerosol



loadings are more representative of atmospheric conditions. More experiments at low organic aerosol loading could be carried out to provide more information. Good performances are also obtained for most of the anthropogenic experiments. However, the experiments with the lower TMB/NO<sub>x</sub> ratio underestimates concentrations by 30 % whereas the experiments with the higher TMB/NO<sub>x</sub> ratio overestimates concentrations by 30 %. This could indicate a more complex NO<sub>x</sub> chemistry than what is taken into account inside the model. However, this discrepancy could be due to the difficulty to simulate properly radicals inside the chamber under some conditions. More experiments should be carried out to confirm these results and improve the NO<sub>x</sub> dependency inside the model.

Oligomerization was shown to have little impact on SOA mass during experiments. However, oligomerization was found to influence composition as a large part of SOA is constituted (more than 50% for biogenic experiments) by oligomers in simulations, especially at low humidity. Moreover, even at high humidities under representative atmospheric conditions, simulations indicate that oligomerization could increase substantially organic aerosol concentrations. However, more efforts should be deployed to improve this parameterization. Indeed, this parameterization represents a “bulk oligomerization” and does not account for differences in the reactivity of monomers. This parameterization could nonetheless be useful to study the effect of oligomerization in 3D air quality models.

The uptake of pinonaldehyde was found to be too slow to contribute significantly to the formation of organic aerosols and that the approach of Pun and Seigneur (2007) greatly overestimates the effect of the particle acidity on SOA formation. However, it could be possible that the uptake of aldehydes less volatile than pinonaldehyde (or more reactive) is strongly influenced by the particle acidity leading to the formation of oligomers or organosulfate. However, the uptake of aldehydes could reach an equilibrium and not be irreversible as assumed in this study. Experiments are needed to confirm those points.

Taking into account wall losses of organic vapors with the parameters of Zhang et al. (2014) leads to a significant underestimation of SOA concentrations up to a factor 3. This feature is not surprising as the mechanism developed in this study was based on experimental results from Teflon chambers and the Odum methodology (Odum et al., 1996) which do not take into wall losses of vapors. This underestimation could however be corrected by decreasing the volatility of SVOC by a factor 3.

However, the experimental conditions do not cover the full range of RH whereas the model shows that RH may strongly influence SOA yields which is consistent with the results of Healy et al. (2009). More experiments need to be carried out at high humidity to confirm the effect of humidity and to validate performances of the model under these conditions.

Finally, these parameterizations should be implemented in a 3D air quality models to evaluate their impact on SOA formation. Oligomerization should especially be studied into greater details as it could lead either to an increase or a decrease (by increasing the mean molar mass that would lead to a decrease of the partitioning constant of monomers) of SOA concentrations. Moreover, different parameterizations of oligomerization could lead to very different results. It is therefore important to determine experimentally the chemical mechanisms involved in SOA formation: first order or second order reaction, complete or equilibrium reaction.

*Acknowledgements.* This work was funded by the French Ministry in charge of ecology.



## References

- Bian, Q., May, A. A., Kreidenweis, S. M., and Pierce, J. R.: Investigation of particle and vapor wall-loss effects on controlled wood-smoke smog-chamber experiments, *Atmos. Chem. and Phys.*, 15, 11 027–11 045, doi:10.5194/acp-15-11027-2015, 2015.
- Carlton, A. G., Bhave, P. V., Napelenok, S. L., Edney, E. O., Sarwar, G., Pinder, R. W., Pouliot, G. A., and Houyoux, M.: Model Representation of Secondary Organic Aerosol in CMAQv4.7, *Environ. Sci. Tech.*, 44, 8553–8560, doi:10.1021/es100636q, 2010.
- 5 Chacon-Madrid, H. J. and Donahue, N. M.: Photo-oxidation of pinonaldehyde at low  $\text{NO}_x$ : from chemistry to organic aerosol formation, *Atmos. Chem. Phys.*, 13, 3277–3236, doi:10.5194/acp-13-3227-2013, 2013.
- Cocker III, D. R., Mader, B. T., Kalberer, M., Flgan, R. C., and H., S. . J.: The effect of water on gas-particle partitioning of secondary organic aerosol: II. m-xylene and 1,3,5-trimethylbenzene photooxidation systems, *Atmos. Environ.*, 35, 6073–6085, doi:10.1016/S1352-10 2310(01)00405-8, 2001.
- Couvidat, F. and Sartelet, K.: The Secondary Organic Aerosol Processor (SOAP v1.0) model: a unified model with different ranges of complexity based on the molecular surrogate approach, *Geosci. Model Dev.*, 8, 1111–1138, doi:10.5194/gmd-8-1111-2015, 2015.
- Couvidat, F. and Seigneur, C.: Modeling secondary organic aerosol formation from isoprene oxidation under dry and humid conditions, *Atmos. Chem. Phys.*, 11, 893–909, doi:10.5194/acp-11-893-2011, 2011.
- 15 Couvidat, F., Debry, É., Sartelet, K., and Seigneur, C.: A Hydrophilic/Hydrophobic Organic ( $\text{H}^2\text{O}$ ) model: Model development, evaluation and sensitivity analysis, *J. Geophys. Res.*, 117, D10 304, doi:10.1029/2011JD017214, 2012.
- DePalma, J. W., Horan, A. J., Hall IV, W. A., and Johnston, M. V.: Thermodynamics of oligomer formation: implications for secondary organic aerosol formation and reactivity, *Phys. Chem. Chem. Phys.*, 15, 6935–6944, doi:10.1039/C3cp44586k, 2013.
- Donahue, N. M., Robinson, A. L., Stanier, C. O., and Pandis, S. N.: Coupled Partitioning, Dilution, and Chemical Aging of Semivolatile 20 Organics, *Environ. Sci. Technol.*, 40, 2635–2643, doi:10.1021/es052297c, 2006.
- Donahue, N. M., Epstein, S. A., Pandis, S. N., and Robinson, A. L.: A two-dimensional volatility basis set: 1. Organic-aerosol mixing thermodynamics, *Atmos. Chem. Phys.*, 11, 3303–3318, doi:doi:10.5194/acp-11-3303-2011, 2011.
- Fountoukis, C. and Nenes, A.: ISORROPIA II: a computationally efficient thermodynamic equilibrium model for  $\text{K}^+$ - $\text{Ca}^{2+}$ - $\text{Mg}^{2+}$ - $\text{NH}_4^+$ - $\text{Na}^+$ - $\text{SO}_4^{2-}$ - $\text{NO}_3^-$ - $\text{Cl}^-$ - $\text{H}_2\text{O}$  aerosols, *Atmos. Chem. Phys.*, 7, 4639–4659, doi:10.5194/acp-7-4639-2007, 2007.
- 25 Fry, J. L., Draper, D. C., Barsanti, K. C., Smith, J. N., Ortega, J., Winkler, P. M., Lawler, M. J., Brown, S. S., Edwards, P. M., Cohen, R. C., and Lee, L.: Secondary Organic Aerosol Formation and Organic Nitrate Yield from  $\text{NO}_3$  Oxidation of Biogenic Hydrocarbons, *Environ. Sci. Technol.*, 48, 11 944–11 953, doi:10.1021/es502204x, 2014.
- Ganbavale, G., Zuend, A., Marcolli, C., and Peter, T.: Improved AIOMFAC model parameterisation of the temperature dependence of activity coefficients for aqueous organic mixtures, *Atmos. Chem. Phys.*, 15, 447–493, doi:10.5194/acp-15-447-2015, 2015.
- 30 Gao, S., Keywood, M., Ng, N. L., Surratt, J., Varutbangkul, V., Bahreini, R., Flagan, R. C., and Seinfeld, J. H.: Low-Molecular-Weight and Oligomeric Components in Secondary Organic Aerosol from the Ozonolysis of Cycloalkenes and  $\alpha$ -pinene, *J. Phys. Chem. A*, 108, 10 147–10 164, doi:10.1021/jp047466e, 2004a.
- Gao, S., Ng, N. L., Keywood, M., Varutbangkul, V., Bahreini, R., Nenes, A., He, J., Yoo, K. Y., Beauchamp, J. L., Hodyss, R. P., Flagan, R. C., and Seinfeld, J. H.: Particle phase acidity and oligomer formation in secondary organic aerosol, *Environ. Sci. Technol.*, 38, 6582–6589, 35 doi:10.1021/es049125k, 2004b.
- Goliff, W. S., Stockwell, W. R., and Lawson, C. V.: The Regional Atmospheric Chemistry Mechanism, Version 2, *Atmos. Environ.*, 68, 174–185, 2013.





- Griffin, R. J., Nguyen, K., Dabdub, D., and Seinfeld, J. H.: A coupled hydrophobic-hydrophilic model for predicting secondary organic aerosol formation, *J. Atmos. Chem.*, 44, 171–190, doi:10.1023/A:1022436813699, 2003.
- Hakola, H., Arey, J., Aschmann, S. M., and Atkinson, R.: Product formation from the gas-phase reactions of OH radicals and O<sub>3</sub> with a series of monoterpenes, *J. Atmos. Chem.*, 18, 75–102, doi:10.1007/BF00694375, 1994.
- 5 Hall IV, W. A. and Johnston, M. V.: Oligomer Content of  $\alpha$ -Pinene Secondary Organic Aerosol, *Aerosol Sci. Tech.*, 45, 37–45, doi:10.1080/02786826.2010.517580, 2011.
- Hallquist, M., Wängberg, I., Ljungström, E., Barnes, I., and Becher, K.-H.: Aerosol and product yield from NO<sub>3</sub> radical-initiated oxidation of selected monoterpenes, *Environ. Sci. Technol.*, 33, 553–559, doi:10.1021/es980292s, 1999.
- Healy, R. M., Temime, B., Kuprovskyyte, K., and Wenger, J. C.: Effect of Relative Humidity on Gas/Particle Partitioning and Aerosol Mass Yield in the Photooxidation of p-Xylene, *Environ. Sci. Technol.*, 43, 1884–1889, doi:10.1021/es802404z, 2009.
- 10 Im, Y., Jang, M., and Beardsley, R. L.: Simulation of aromatic SOA formation using the lumping model integrated with explicit gas-phase kinetic mechanisms and aerosol-phase reactions, *Atmos. Chem. Phys.*, 14, 4013–4027, doi:10.5194/acp-14-4013-2014, 2014.
- Jathar, S. H., Cappa, C. D., Wexler, A. S., Seinfeld, J. H., and Kleeman, M. J.: Multi-generational oxidation model to simulate secondary organic aerosol in a 3-D air quality model, *Geosci. Model Dev.*, 8, 2253–2567, doi:10.5194/gmd-8-2553-2015, 2015.
- 15 Jenkin, M. E., Saunders, S. M., and Pilling, M. J.: The tropospheric degradation of volatile organic compounds: a protocol for mechanism development, *Atmos. Environ.*, 31, 81–104, 1997.
- Kalberer, M., Paulsen, D., Sax, M., Steinbacher, M., Dommen, J., Prevot, A. S. H., Fisseha, R., Weingartner, E., Frankevich, V., Zenobi, R., and Baltensperger, U.: Identification of Polymers as Major Components of Atmospheric Organic Aerosols, *Science*, 303, 1659–1662, doi:10.1126/science.1092185, 2004.
- 20 Kalberer, M., Sax, M., and Samburova, V.: Molecular size evolution of oligomers in organic aerosols collected in urban atmospheres and generated in a smog chamber, *Environ. Sci. Technol.*, 40, 5917–5922, doi:10.1021/es0525760, 2006.
- Kanakidou, M., Seinfeld, J. H., Pandis, S. N., Barnes, I., Dentener, F. J., Facchini, M. C., Van Dingenen, R., Ervens, B., Nenes, A., Nielsen, C. J., Swietlicki, E., Putaud, J. P., Balkanski, Y., Fuzzi, S., Horth, J., Moortgat, G. K., Winterhalter, R., Myhre, C. E. L., Tsigaridis, K., Vignati, E., Stephanou, E. G., and Wilson, J.: Organic aerosol and global climate modelling: a review, *Atmos. Chem. Phys.*, 5, 1053–1123, doi:10.5194/acp-5-1053-2005, 2005.
- 25 Keene, W. C., Pszenny, A. A. P., Maben, J. R., Stevenson, E., and Wall, A.: Closure evaluation of size-resolved aerosol pH in the New England coastal atmosphere during summer, *J. Geophys. Res.*, 109, D23 307, doi:10.1029/2004JD004801, 2004.
- Kim, H., Liu, S., Russell, J. M., and Paulson, S. E.: Dependence of Real Refractive Indices on O:C, H:C and Mass Fragments of Secondary Organic Aerosol Generated from Ozonolysis and Photooxidation of Limonene and  $\alpha$ -Pinene, *Aerosol Sci. and Tech.*, 48, 498–507, doi:10.1080/02786826.2014.893278, 2014.
- 30 Kim, Y., Sartelet, K., and Seigneur, C.: Comparison of two gas-phase chemical kinetic mechanisms of ozone formation over Europe, *J. Atmos. Chem.*, 62, 82–119, doi:10.1007/s10874-009-9142-5, 2009.
- Kristensen, K., Cui, T., Zhang, H., Gold, A., Glasius, M., and Surratt, J. D.: Dimers in  $\alpha$ -pinene secondary organic aerosol: effect of hydroxyl radical, ozone, relative humidity and aerosol acidity, *Atmos. Chem. Phys.*, 14, 4201–4218, doi:10.5194/acp-14-4201-2014, 2014.
- 35 Lee, B.-H., Pierce, J. R., Engelhart, G. J., and Pandis, S. N.: Volatility of secondary organic aerosol from the ozonolysis of monoterpenes, *Atmos. Environ.*, 45, 2443–2452, doi:10.1016/j.atmosenv.2011.02.004, 2011.
- Lemaire, V., Coll, I., Couvidat, F., Mouchel-Vallon, C., Seigneur, C., and Siour, G.: Oligomer formation in the troposphere: from experimental knowledge to 3-D modeling, *Geosci. Model Dev. Discuss*, 8, 9229–9279, doi:10.5194/gmdd-8-9229-2015, 2015.



- Liggio, J. and Li, S.-M.: Organosulfate formation during the uptake of pinonaldehyde on acidic sulfate aerosols, *Geophys. Res. Lett.*, 33, L13 808, doi:10.1029/2006GL026079, 2006a.
- Liggio, J. and Li, S.-M.: Reactive uptake of pinonaldehyde on acidic aerosols, *J. Geophys. Res.*, 111, 1111–1138, doi:10.1029/2005JD006978, 2006b.
- 5 Lim, Y. B. and Ziemann, P. J.: Products and Mechanism of Secondary Organic Aerosol Formation from Reactions of n-Alkanes with OH Radicals in the Presence of NO<sub>x</sub>, *Environ. Sci. Technol.*, 39, 9229–9236, doi:10.1021/es051447g, 2005.
- Ludwig, J. and Klemm, O.: Acidity of size-fractionated aerosol particles, *Water Air Soil Pollut*, 49, 35–50, doi:10.1007/BF00279508, 1990.
- Madon, R. J. and Iglesia, E.: Catalytic reaction rates in thermodynamically non-ideal systems, *J. Mol. Catal. A*, 163, 189–204, 2000.
- Menut, L., Bessagnet, B., Khvorostyanov, D., Beekmann, M., Blond, N., Colette, A., Coll, I., Curci, G., Foret, G., Hodzic, A., Mailler, S.,  
10 Meleux, F., Monge, J.-L., Pison, I., Siour, G., Turquety, S., Valari, M., Vautard, R., and Vivanco, M. G.: CHIMERE 2013: a model for regional atmospheric composition modelling, *Geosci. Model Dev.*, 6, 981–1028, doi:10.5194/gmd-6-981-2013, 2013.
- Müller, L., Naumann, K. H., Saathoff, H., Mentek, T. F., and Donahue, N. M.: Formation of 3-methyl-1,2,3-butanetricarboxylic acid via gas phase oxidation of pinonic acid - a mass spectrometric study of SOA aging, *Atmos. Chem. Phys.*, 12, 1483–1496, doi:10.5194/acp-12-1483-2012, 2012.
- 15 Mutzel, A., Rodigast, M., Iinuma, Y., Böge, O., and Herrmann, H.: Monoterpene SOA - Contribution of first-generation oxidation products to formation and chemical composition, *Atmos. Environ.*, 130, 136–144, doi:10.1016/j.atmosenv.2015.10.080, 2016.
- Ng, N. L., Chhabra, P. S., Chan, A. W. H., Surratt, J. D., Kroll, J. H., Kwan, A. J., McCabe, D. C., Wennberg, P. O., Sorooshian, A., Murphy, S. M., Dalleska, N. F., Flagan, R. C., and Seinfeld, J. H.: Effect of NO<sub>x</sub> level on secondary organic aerosol (SOA) formation from the photooxidation of terpenes, *Atmos. Chem. Phys.*, 7, 5159–5174, doi:10.5194/acp-7-5159-2007, 2007a.
- 20 Ng, N. L., Kroll, J. H., Chan, A. W. H., Chhabra, P. S., Flagan, R. C., and Seinfeld, J. H.: Secondary organic aerosol formation from m-xylene, toluene, and benzene, *Atmos. Chem. Phys.*, 7, 3909–3922, doi:10.5194/acp-7-3909-2007, 2007b.
- Odum, J. R., Hoffmann, F., Bowman, D., Collins, D., Flagan, R. C., and Seinfeld, J. H.: Gas/particle partitioning and secondary organic aerosol yields, *Environ. Sci. Technol.*, 30, 2580–2585, doi:10.1021/es950943+, 1996.
- Pankow, J. F.: An absorption model of gas/particle partitioning of organic compounds in the atmosphere, *Atmos. Environ.*, 28A, 185–188,  
25 1994.
- Pun, B. K. and Seigneur, C.: Investigative modeling of new pathways for secondary organic aerosol formation, *Atmos. Chem. Phys.*, 7, 2199–2216, doi:10.5194/acp-7-2199-2007, 2007.
- Pun, B. K., Griffin, R. J., Seigneur, C., and Seinfeld, J. H.: Secondary organic aerosol. 2. Thermodynamic model for gas/particle partitioning of molecular constituents, *J. Geophys. Res.*, 107, 433, doi:10.1029/2001JD000542, 2002.
- 30 Pun, B. K., Seigneur, C., and Lohman, K.: Modeling secondary organic aerosol formation via multiphase partitioning with molecular data, *Environ. Sci. Technol.*, 40, 4722–4731, doi:10.1021/es0522736, 2006.
- Rahimpour, M. R.: A non-ideal rate-based model for industrial urea thermal hydrolyser, *Chem. Eng. Process.*, 43, 1299–1307, doi:10.1016/j.cep.2003.12.005, 2004.
- Roldin, P., Eriksson, A. C., Nordin, E. Z., Hermansson, E., Mogensen, D., Rusanen, A., Boy, M., Swietlicki, E., Svenningsson, B., Zelenyuk, A., and Pagels, J.: Modelling non-equilibrium secondary organic aerosol formation and evaporation with the aerosol dynamics, gas- and particle-phase chemistry kinetic multilayer model ADCHAM, *Atmos. Chem. Phys.*, 14, 7953–7993, doi:10.5194/acp-14-7953-2014, 2014.



- Santiago, M., Vivanco, M. G., and Stein, A. F.: Evaluation of CMAQ parameterizations for SOA formation from the photooxidation of alpha-pinene and limonene against smog chamber data, *Atmos. Environ.*, 56, 236–245, doi:10.1016/j.atmosenv.2012.04.011, 2012.
- Sato, K., Takami, A., Kato, Y., Seta, T., Fujitani, Y., Hikida, T., Shimono, A., and Imamura, T.: AMS and LC/MS analyses of SOA from the photooxidation of benzene and 1,3,5-trimethylbenzene in the presence of NO<sub>x</sub>: effects of chemical structure on SOA aging, *Atmos. Chem. Phys.*, 12, 4667–4682, doi:10.5194/acp-12-4667-2012, 2012.
- 5 Sato, K., Jia, T., Tanabe, K., Morino, Y., Yoshizumi Kajii, Y., and Imamura, T.: Terpenylic acid and nine-carbon multifunctional compounds formed during the aging of  $\beta$ -pinene ozonolysis secondary organic aerosol, *Atmos. Environ.*, 130, 127–135, doi:10.1016/j.atmosenv.2015.08.047, 2016.
- Saunders, S. M., Jenkin, M. E., Derwent, R. G., and Pilling, M. J.: Protocol for the development of the Master Chemical Mechanism, MCM v3 (Part A): tropospheric degradation of non-aromatic volatile organic compounds, *Atmos. Chem. Phys.*, 3, 161–180, doi:10.5194/acp-3-161-2003, 2003.
- 10 Schell, B., Ackermann, I. J., Hass, H., Binkowski, F. S., and Ebel, A.: Modeling the formation of secondary organic aerosol within a comprehensive air quality model system, *J. Geophys. Res.*, 106, 28 275–28 293, doi:10.1029/2001JD000384, 2001.
- Schilling, K. A.: Secondary Organic Aerosol Composition Studies Using Mass Spectrometry, Ph.D. thesis, California Institute of Technology, doi:10.7907/Z93F4MJR, 2015.
- 15 Seinfeld, J. and Pandis, S.: Atmospheric chemistry and physics: from air pollution to climate change, Wiley-interscience, 1998.
- Song, M., Liu, P. F., Hanna, S. J., Zaveri, R. A., Potter, K., You, Y., Martin, S. T., and Bertram, A. K.: Relative humidity-dependent viscosity of secondary organic material from toluene photo-oxidation and possible implications for organic particulate matter over megacities, *Atmos. Chem. Phys.*, 16, 8817–8830, doi:10.5194/acp-16-8817-2016, 2016.
- 20 Surratt, J. D., Murphy, S. M., Kroll, J. H., Ng, N. L., Hildebrandt, L., Sorooshian, A., Szmigielski, R., Vermeulen, R., Maenhaut, W., Claeys, M., Flagan, R. C., and Seinfeld, J. H.: Chemical composition of secondary organic aerosol formed from the photooxidation of isoprene, *J. Phys. Chem. A*, 110, 9665–9690, doi:10.1021/jp061734m, 2006.
- Svendby, T. M., Lazaridis, M., and Tørseth, K.: Temperature dependent secondary organic aerosol formation from terpenes and aromatics, *J. Atmos. Chem.*, 59, 25–46, doi:10.1007/s10874-007-9093-7, 2008.
- 25 Trump, E. R. and Donahue, N. M.: Oligomer formation within secondary organic aerosols: equilibrium and dynamic considerations, *Atmos. Chem. Phys.*, 14, 3691–3701, doi:10.5194/acp-14-3691-2014, 2014.
- Tulet, P., Grini, A., Griffin, R. J., and Petitcol, S.: ORILAM-SOA: A computationally efficient model for predicting secondary organic aerosols in three-dimensional atmospheric models, *J. Geophys. Res.*, 111, D23 208, doi:10.1029/2006JD007152, 2006.
- Verwer, J. G., Spee, E. J., Bloom, J. G., and Hundsdorfer, W.: A second-order rosenbrock method applied to photochemical dispersion problems, *SIAM J. Sci. Comput.*, 20, 1456–1480, doi:10.1137/S1064827597326651, 1999.
- 30 Vivanco, M. G., Santiago, M., Martínez-Tarifa, A., Borrás, E., Ródenas, M., García-Diego, C., and Sánchez, M.: SOA formation in a photoreactor from a mixture of organic gases and HONO for different experimental conditions, *Atmos. Environ.*, 45, 708–715, doi:10.1016/j.atmosenv.2010.09.059, 2011.
- Vivanco, M. G., Santiago, M., Sánchez, M., Clavero, M. A., Borrás, E., Ródenas, M., Alacreu, F., Vásquez, M., Clemente, E., Porras, R., Muñoz, A., and Stein, A.: Experimental data on SOA formation from mixtures of anthropogenic and biogenic organic compounds, *Atmósfera*, 26, 59–73, 2013.



- Vivanco, M. G., Couvidat, F., Seigneur, C., Jang, M., Santiago, M., and Bessagnet, B.: Evaluation of some SOA formation schemes for the oxidation of anthropogenic gases against experiments in two outdoor chambers, *International Journal of Environment and Pollution*, 59, 43–55, doi:10.1504/IJEP.2016.078062, 2016.
- Volkamer, R., Platt, U., and Wirtz, K.: Primary and secondary glyoxal formation from aromatics: experimental evidence for the bicycloalkyl-radical pathway from benzene, toluene, and p-xylene, *J. Phys. Chem. A*, 105, 7865–7874, doi:10.1021/jp010152w, 2001.
- WHO: Health Aspects of Air Pollution with Particulate Matter, Ozone and Nitrogen Dioxide, Tech. rep., WHO EUR/03/5042688, 2003.
- Yu, S., Bhawe, P. V., Dennis, R. L., and Marthur, R.: Seasonal and regional variations of primary and secondary organic aerosols over the Continental United States: Semi-empirical estimates and model evaluation, *Environ. Sci. Technol.*, 41, 4690–4697, doi:10.1021/es061535g, 2007.
- 10 Zhang, Q., Jimenez, J. L., Canagaratna, M. R., Allan, J. D., Coe, H., Ulbrich, I., Alfarra, M. R., Takami, A., Middlebrook, A. M., Sun, Y. L., Dzepina, K., Dunlea, E., Docherty, K., De-Carlo, P. F., Salcedo, D., Onasch, T., Jayne, J. T., Miyoshi, T., Shimojo, A., Hatakeyama, S., Takegawa, N., Kondo, Y., Schneider, J., Drewnick, F., Borrmann, S., Weimer, S., Demerjian, K., Williams, P., Bower, K., Bahreini, R., Cottrell, L., Griffin, R. J., Rautiainen, J., Sun, J. Y., Zhang, Y. M., and Worsnop, D. R.: Ubiquity and dominance of oxygenated species in organic aerosols in anthropogenically-influenced Northern Hemisphere midlatitudes, *Geophys. Res. Lett.*, 34, L13 801, doi:10.1029/2007GL029979, 2007.
- 15 Zhang, X., Cappa, C. D., Jathar, S. H., McVay, R. C., Ensberg, J. J., Kleeman, M. J., and Seinfeld, J. H.: Influence of vapor wall loss in laboratory chambers on yields of secondary organic aerosol, *Proc. Natl. Acad. Sci.*, 111, 5802–5807, doi:10.1073/pnas.1404727111, 2014.
- Zhang, X., Schwantes, R. H., McVay, R. C., Lignell, H., Coggon, M. M., Flagan, R. C., and Seinfeld, J. H.: Vapor wall deposition in Teflon chambers, *Atmos. Chem. Phys.*, 15, 4197–4214, doi:10.5194/acp-15-4197-2015, 2015.
- 20 Zuend, A. and Seinfeld, J. H.: Modeling the gas-particle partitioning of secondary organic aerosol: the importance of liquid-liquid phase separation, *Atmos. Chem. Phys.*, 12, 3857–3882, doi:10.5194/acp-12-3857-2012, 2012.
- Zuend, A., Marcolli, C., Luo, B. P., and Peter, T.: A thermodynamic model of mixed organic-inorganic aerosols to predict activity coefficients, *Atmos. Chem. Phys.*, 8, 4559–4593, doi:10.5194/acp-8-4559-2008, 2008.
- 25 Zuend, A., Marcolli, C., Booth, A. M., Lienhard, D. M., Soonsin, V., Krieger, U. K., Topping, D. O., McFiggans, G., Peter, T., and Seinfeld, J. H.: New and extended parameterization of the thermodynamic model AIOMFAC: calculation of activity coefficients for organic-inorganic mixtures containing carboxyl, hydroxyl, carbonyl, ether, ester, alkenyl, alkyl, and aromatic functional groups, *Atmos. Chem. Phys.*, 11, 9155–9206, doi:10.5194/acp-11-9155-2011, 2011.



**Table 1.** Initial concentrations in ppb, temperature (T) in Kelvin and relative humidity in % for biogenic experiments.

| Experiment | Isoprene | $\alpha$ -pinene | Limonene | NO  | NO <sub>2</sub> | HONO | SO <sub>2</sub> | T       | RH    |
|------------|----------|------------------|----------|-----|-----------------|------|-----------------|---------|-------|
| B1         | 107      | 66               | 58       | 34  | 128             | 99   | 0               | 302-307 | 0.5-3 |
| B2         | 92       | 50               | 50       | 48  | 0               | 87   | 0               | 298-300 | 30-26 |
| B3         | 122      | 71               | 40       | 41  | 0               | 53   | 0               | 297-300 | 19-22 |
| B4         | 0        | 63               | 65       | 32  | 0               | 101  | 0               | 294-298 | 8-13  |
| B5         | 99       | 59               | 53       | 150 | 0               | 307  | 0               | 295-297 | 8-11  |
| B6         | 87       | 50               | 51       | 244 | 89              | 40   | 513             | 295-300 | 15-19 |
| B7         | 55       | 79               | 76       | 198 | 0               | 165  | 461             | 302-305 | 20-30 |

**Table 2.** Initial concentrations in ppb, temperature (T) in Kelvin and relative humidity in % for anthropogenic experiments. SO<sub>2</sub> was not present for those experiments.

| Experiment | Toluene | Xylene | TMB | Octane | NO | NO <sub>2</sub> | HONO | T       | RH    |
|------------|---------|--------|-----|--------|----|-----------------|------|---------|-------|
| A1         | 102     | 22     | 153 | 85     | 19 | 0               | 99   | 299-305 | 10-16 |
| A2         | 200     | 49     | 300 | 155    | 23 | 0               | 75   | 302-305 | 9-18  |
| A3         | 48      | 11     | 106 | 42     | 23 | 0               | 71   | 302-307 | 6-14  |
| A4         | 98      | 24     | 160 | 79     | 37 | 0               | 156  | 297-307 | 6-13  |
| A5         | 97      | 21     | 146 | 81     | 4  | 8               | 52   | 297-308 | 7-14  |
| A6         | 93      | 22     | 146 | 78     | 21 | 0               | 94   | 300-308 | 0.4   |
| A7         | 107     | 26     | 160 | 89     | 21 | 0               | 89   | 306-309 | 7-10  |
| A8         | 116     | 29     | 19  | 10     | 57 | 0               | 119  | 302-305 | 15-18 |
| A9         | 81      | 21     | 118 | 65     | 31 | 0               | 90   | 299-303 | 28-37 |

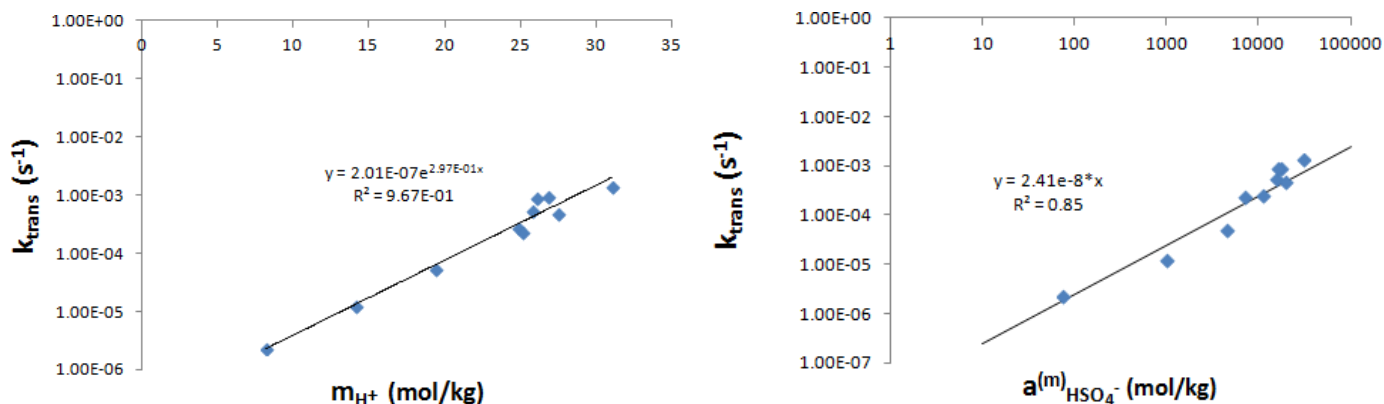


**Figure 1.** Kinetic rate of transformation of pinonaldehyde as a function of  $m_{H^+}$  the molality of ion  $H^+$  (left) and  $a_{HSO_4^-}^{(m)}$  the activity as a molality basis of ion  $HSO_4^-$  (right).



**Table 3.** Reactions leading to SOA formation<sup>a</sup> from  $\alpha$ -pinene,  $\beta$ -pinene and limonene.

| Reaction  | Kinetic rate parameter (molecule <sup>-1</sup> .cm <sup>3</sup> .s <sup>-1</sup> ) |
|---|--|
| API + OH → 0.30 BiA0D + 0.40 BiA2D + OH   | $1.21 \times 10^{-11} \times \exp\left(\frac{440}{T}\right)$                       |
| API + O <sub>3</sub> → APIO3RAD + O <sub>3</sub>  | $5.00 \times 10^{-16} \times \exp\left(\frac{-530}{T}\right)$                      |
| APIO3RAD + HO <sub>2</sub> → 0.024 BiA3D + 0.15 BiA2D + 0.38 BiA1D + HO <sub>2</sub>                        | $4.10 \times 10^{-13} \times \exp\left(\frac{790}{T}\right)$                       |
| APIO3RAD + NO → 0.085 BiA2D + 0.24 BiA1D + NO   | $8.8 \times 10^{-13} \times \exp\left(\frac{180.2}{T}\right)$                      |
| API + NO <sub>3</sub> → 0.70 BiA0D + NO <sub>3</sub>  | $1.19 \times 10^{-12} \times \exp\left(\frac{-490}{T}\right)$                      |
| BPI + OH → 0.07 BiA0D + 0.08 BiA1D + 0.06 BiA2D + 0.27 NOPINONE + OH  | $2.38 \times 10^{-11} \times \exp\left(\frac{357}{T}\right)$                       |
| BPI + O <sub>3</sub> → 0.09 BiA0D + 0.022 BiA3D + 0.045 BiA2D + 0.20 BiA1D + 0.17 NOPINONE + O <sub>3</sub> | $1.50 \times 10^{-17}$   |
| BPI + NO <sub>3</sub> → 0.02 BiA0D + 0.21 BiNIT + 0.02 NOPINONE + NO <sub>3</sub>                           | $2.51 \times 10^{-12}$   |
| LIM + OH → 0.35 BiA0D + 0.15 BiA2D + OH   | $4.20 \times 10^{-11} \times \exp\left(\frac{401}{T}\right)$                       |
| LIM + O <sub>3</sub> → LIMO3RAD + O <sub>3</sub>  | $2.95 \times 10^{-15} \times \exp\left(\frac{783}{T}\right)$                       |
| LIMO3RAD + HO <sub>2</sub> → 0.14 BiA3D + 0.44 BiA2D + 0.42 BiA1D + HO <sub>2</sub>                         | $4.10 \times 10^{-13} \times \exp\left(\frac{790}{T}\right)$                       |
| LIMO3RAD + NO → 0.14 BiA3D + 0.5 BiA2D + 0.36 BiA1D + NO  | $8.8 \times 10^{-13} \times \exp\left(\frac{180.2}{T}\right)$                      |
| LIM + NO <sub>3</sub> → 0.69 BiA0D + 0.28 BiNIT + NO <sub>3</sub>   | $1.22 \times 10^{-11}$   |

<sup>a</sup> Oxidants may be present as both reactants and products so that a reaction added to RACM2 will not affect the original photochemical oxidant concentrations. MO<sub>2</sub> and ACO<sub>3</sub> are the methylperoxy radical and the peroxy-acetyl radical respectively. A is either NO, NO<sub>3</sub>, MO<sub>2</sub> or ACO<sub>3</sub>.



**Table 4.** Reactions leading to SOA formation<sup>a</sup> from toluene.

| Reaction   | Kinetic rate parameter (molecule <sup>-1</sup> .cm <sup>3</sup> .s <sup>-1</sup> )   |
|--|--|
| TOL + OH → ... + 0.25 TOLP + OH  | $1.80 \times 10^{-12} \times \exp\left(\frac{355}{T}\right)$   |
| TOLP + HO <sub>2</sub> → TOLlowNO <sub>x</sub> + HO <sub>2</sub>                           | $3.75 \times 10^{-13} \times \exp\left(\frac{980}{T}\right)$   |
| TOLP + A → TOLhighNO <sub>x</sub> + A  | A = NO: $2.70 \times 10^{-12} \times \exp\left(\frac{360}{T}\right)$<br>A = NO <sub>3</sub> : $1.2 \times 10^{-12}$<br>A = MO <sub>2</sub> : $3.56 \times 10^{-14} \times \exp\left(\frac{708}{T}\right)$<br>A = ACO <sub>3</sub> : $7.40 \times 10^{-13} \times \exp\left(\frac{765}{T}\right)$ |
| TOLlowNO <sub>x</sub> + OH → TOLlowNO <sub>x</sub> RAD + OH                                | $6.90 \times 10^{-11}$   |
| TOLhighNO <sub>x</sub> + OH → TOLlowNO <sub>x</sub> RAD + OH                               | $6.90 \times 10^{-11}$   |
| TOLlowNO <sub>x</sub> RAD + HO <sub>2</sub> → 0.697 AnPER + HO <sub>2</sub>                | See TOLP + HO <sub>2</sub> reaction  |
| TOLlowNO <sub>x</sub> RAD + A → 0.131 AnRP2 + 0.324 AnIP1 + A                              | See TOLP + A reaction  |
| TOLhighNO <sub>x</sub> RAD + HO <sub>2</sub> → 0.131 AnRP2 + 0.324 AnIP1 + HO <sub>2</sub> | See TOLP + HO <sub>2</sub> reaction  |
| TOLhighNO <sub>x</sub> RAD + A → 0.131 AnRP2 + 0.324 AnIP1 + A                             | See TOLP + A reaction  |

<sup>a</sup> Oxidants may be present as both reactants and products so that a reaction added to RACM2 will not affect the original photochemical oxidant concentrations. MO<sub>2</sub> and ACO<sub>3</sub> are the methylperoxy radical and the peroxy-acetyl radical respectively. A is either NO, NO<sub>3</sub>, MO<sub>2</sub> or ACO<sub>3</sub>.



**Table 5.** Reactions leading to SOA formation<sup>a</sup> from xylene and trimethylbenzene.

| Reaction   | Kinetic rate parameter (molecule <sup>-1</sup> .cm <sup>3</sup> .s <sup>-1</sup> ) |
|--|--|
| XYL + OH → ... + 0.274 XYLP  | $1.70 \times 10^{-11} \times \exp(\frac{116}{T})$                                  |
| XYLP + HO <sub>2</sub> → XYLlowNOx + HO <sub>2</sub>                           | See TOLP + HO <sub>2</sub> reaction  |
| XYLP + A → XYLhighNOx + A  | See TOLP + A reaction  |
| XYLlowNOx + OH → XYLlowNOxRAD + OH   | $6.90 \times 10^{-11}$   |
| XYLhighNOx + OH → XYLlowNOxRAD + OH  | $6.90 \times 10^{-11}$   |
| XYLlowNOxRAD + HO <sub>2</sub> → 0.611 AnPER + HO <sub>2</sub>                 | See TOLP + HO <sub>2</sub> reaction  |
| XYLlowNOxRAD + A → 0.0529 AnRP1 + 0.344 AnIP2 + A                              | See TOLP + A reaction  |
| XYLhighNOxRAD + HO <sub>2</sub> → 0.0529 AnRP1 + 0.344 AnIP2 + HO <sub>2</sub> | See TOLP + HO <sub>2</sub> reaction  |
| XYLhighNOxRAD + A → 0.0529 AnRP1 + 0.344 AnIP2 + A                             | See TOLP + A reaction  |
| TMB + OH → ... + 0.274 TMBP  | $5.67 \times 10^{-11}$   |
| TMBP + HO <sub>2</sub> → TMBlowNOx + HO <sub>2</sub>                           | See TOLP + HO <sub>2</sub> reaction  |
| TMBP + A → TMBhighNOx + A  | See TOLP + A reaction  |
| TMBlowNOx + OH → TMBlowNOxRAD + OH   | $6.90 \times 10^{-11}$   |
| TMBhighNOx + OH → TMBlowNOxRAD + OH  | $6.90 \times 10^{-11}$   |
| TMBlowNOxRAD + HO <sub>2</sub> → 0.611 AnPER + HO <sub>2</sub>                 | See TOLP + HO <sub>2</sub> reaction  |
| TMBlowNOxRAD + A → 0.0117 AnRP1 + 0.250 AnIP2 + A                              | See TOLP + A reaction  |
| TMBhighNOxRAD + HO <sub>2</sub> → 0.0117 AnRP1 + 0.250 AnIP2 + HO <sub>2</sub> | See TOLP + HO <sub>2</sub> reaction  |
| TMBhighNOxRAD + A → 0.0117 AnRP1 + 0.250 AnIP2 + A                             | See TOLP + A reaction  |

<sup>a</sup> Oxidants may be present as both reactants and products so that a reaction added to RACM2 will not affect the original photochemical oxidant concentrations. MO<sub>2</sub> and ACO<sub>3</sub> are the methylperoxy radical and the peroxy-acetyl radical respectively. A is either NO, NO<sub>3</sub>, MO<sub>2</sub> or ACO<sub>3</sub>.



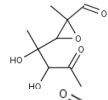
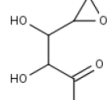
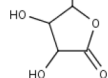
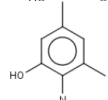
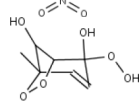
**Table 6.** Aging mechanism of SVOCs<sup>a</sup>.

| Reaction   | Kinetic rate parameter (molecule <sup>-1</sup> .cm <sup>3</sup> .s <sup>-1</sup> ) |
|--|--|
| BiA0D + OH → RA0D + OH                           | $9.0 \times 10^{-12}$  |
| RA0D + HO <sub>2</sub> → BiA1D + HO <sub>2</sub> | $5.20 \times 10^{-13} \times \exp\left(\frac{980}{T}\right)$                       |
| RA0D + NO → 0.6 BiA1D + 0.075 BiA3D + NO         | $7.50 \times 10^{-12} \times \exp\left(\frac{290}{T}\right)$                       |
| BiA1D + OH → 0.061 BiA3D + OH                    | $1.12 \times 10^{-11}$   |
| BiA2D + OH → 0.4 BiA3D + OH                      | $7.29 \times 10^{-12}$   |
| NOPINONE + OH → 0.16 BiA3D + OH                  | $1.55 \times 10^{-11}$   |
| AnRP1 + OH → 0.26 AnRP1a + OH                    | $6.0 \times 10^{-12}$  |
| AnRP2 + OH → 0.06 AnRP2a + OH                    | $6.0 \times 10^{-12}$  |
| AnIP1 + OH → 0.04 AnIP1a + OH                    | $6.0 \times 10^{-12}$  |
| AnIP1a + OH → Volatile products + OH             | $6.0 \times 10^{-12}$  |
| AnIP2 + OH → 0.48 AnIP2a + OH                    | $6.0 \times 10^{-12}$  |
| AnIP2a + OH → 0.38 AnIP2b + OH                   | $6.0 \times 10^{-12}$  |

<sup>a</sup> Oxidants may be present as both reactants and products so that a reaction added to RACM2 will not affect the original photochemical oxidant concentrations. MO<sub>2</sub> and ACO<sub>3</sub> are the methylperoxy radical and the peroxyacetyl radical respectively.



**Table 7.** Properties of the different surrogate SOA species.

| Surrogate | Molecular structure   | MW <sup>a</sup> | $p^0$ <sup>b</sup>    | $\Delta H_{\text{vap}}$ <sup>c</sup> |
|-----------|---|-----------------|-----------------------|--------------------------------------|
| AnRP1     |    | 202             | $1.01 \times 10^{-7}$ | 50                                   |
| AnRP2     |    | 160             | $2.68 \times 10^{-7}$ | 50                                   |
| AnIP1     |   | 132             | $2.36 \times 10^{-6}$ | 50                                   |
| AnIP2     |  | 167             | $1.24 \times 10^{-5}$ | 50                                   |
| AnPER     |  | 190             | non-volatile          | -                                    |
| AnRP1a    | AnRP1 + 1 group OH  | 218             | non-volatile          | -                                    |
| AnRP2a    | AnRP2 + 1 group OH  | 176             | non-volatile          | -                                    |
| AnIP1a    | AnIP1 + 1 group OH  | 148             | $1.36 \times 10^{-7}$ | 50                                   |
| AnIP2a    | AnIP2 + 1 group OH  | 183             | $2.58 \times 10^{-7}$ | 50                                   |
| AnIP2b    | AnIP2a + 1 group OH   | 199             | $5.39 \times 10^{-9}$ | 50                                   |
| BiA0D     | pinonaldehyde   | 168             | $1.0 \times 10^{-3}$  | 50                                   |
| BiA1D     | pinonic acid  | 184             | $5.61 \times 10^{-5}$ | 50                                   |
| BiA2D     | pinic acid  | 186             | $1.67 \times 10^{-6}$ | 50                                   |
| BiA3D     | 3-methyl-1,2,3-butanetricarboxylic acid   | 202             | non-volatile          | -                                    |

<sup>a</sup> Molecular weight [g.mol<sup>-1</sup>]

<sup>b</sup> Saturation vapor pressure [torr] at 298K

<sup>c</sup> Enthalpy of vaporization [kJ.mol<sup>-1</sup>]

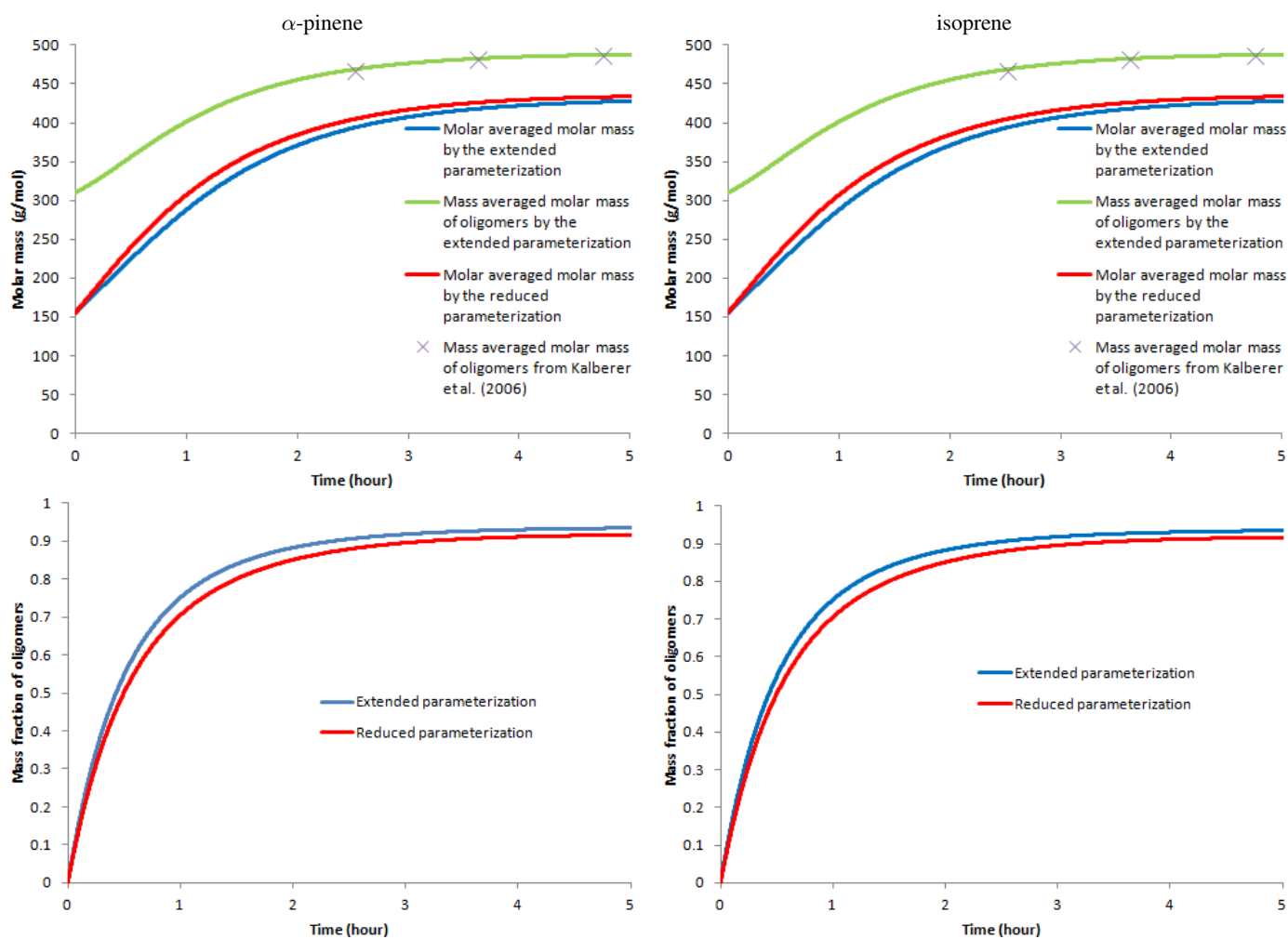


**Figure 2.** Temporal evolution of molar masses (top) and of the mass fraction of oligomer (down) for the extended and reduced parameterizations.

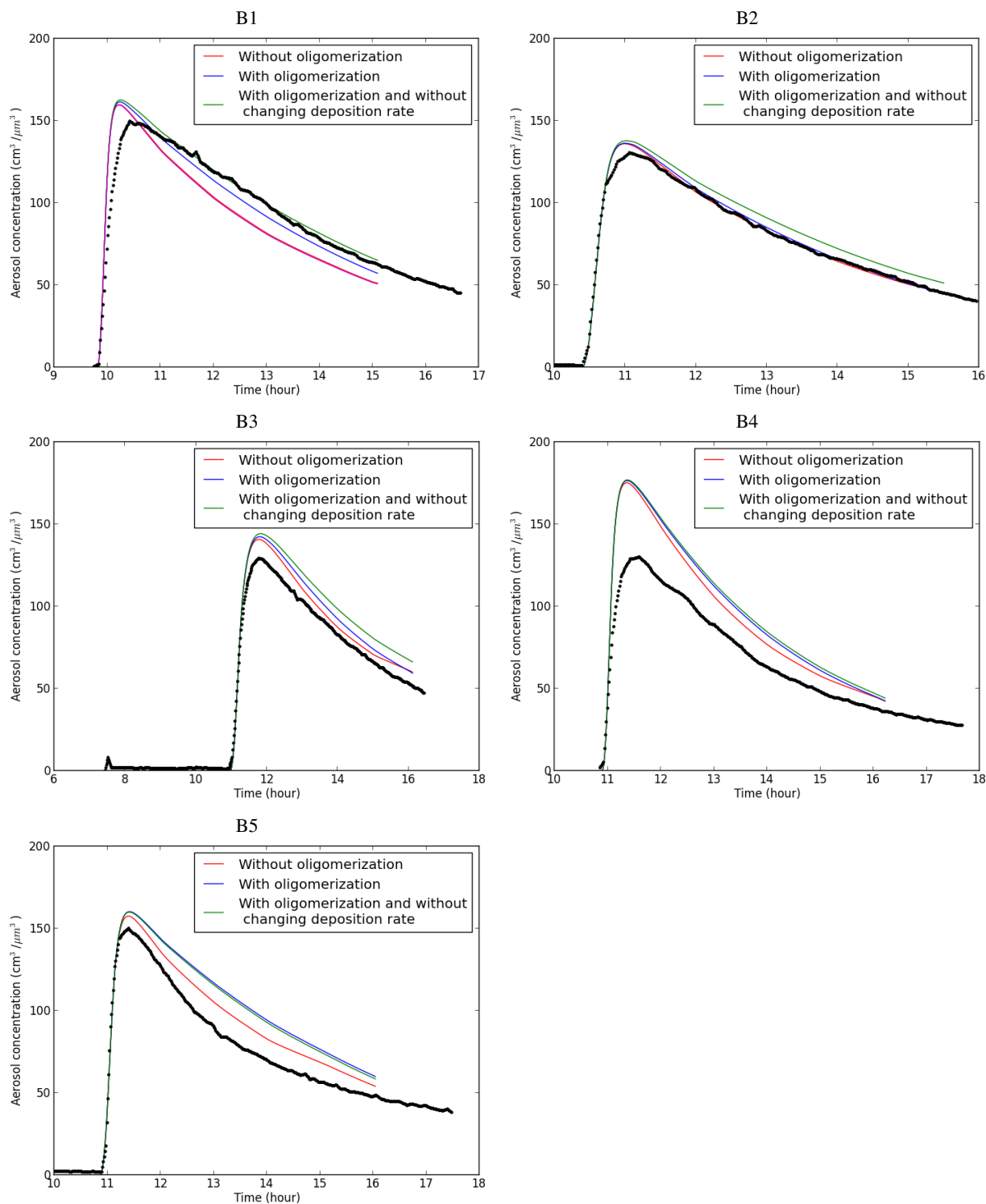


**Figure 3.** Aerosol concentration formation for the biogenic experiments without  $\text{SO}_2$ . Black lines correspond to SMPS measurements.

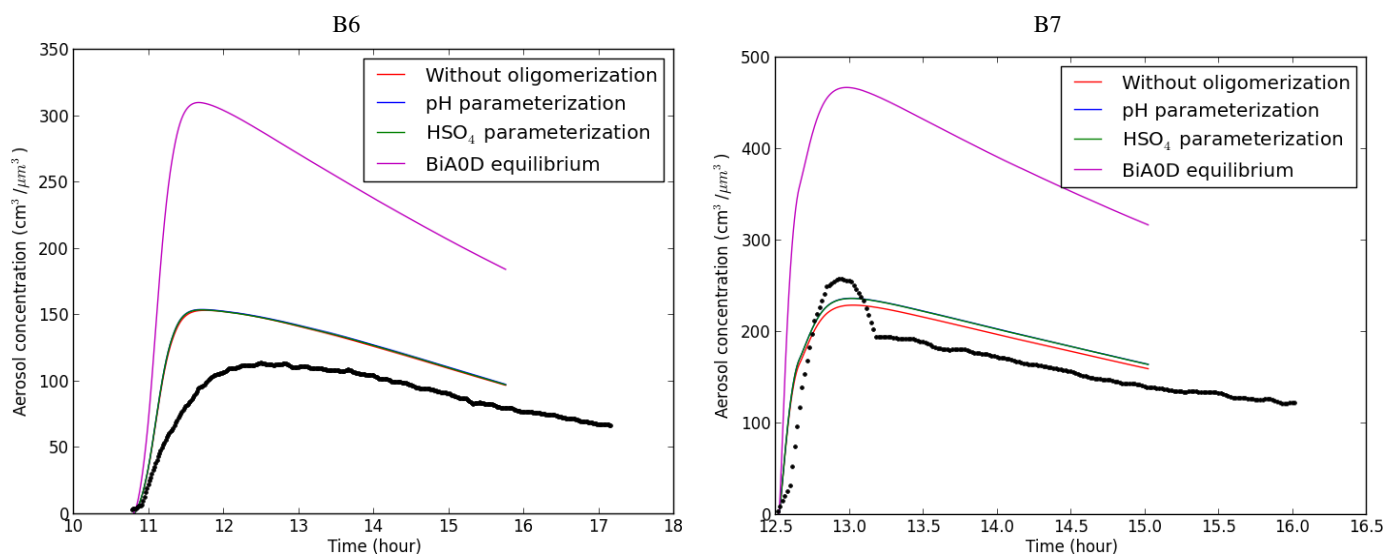


**Figure 4.** Aerosol concentration formation for the biogenic experiments with SO<sub>2</sub>. Black lines correspond to SMPS measurements.

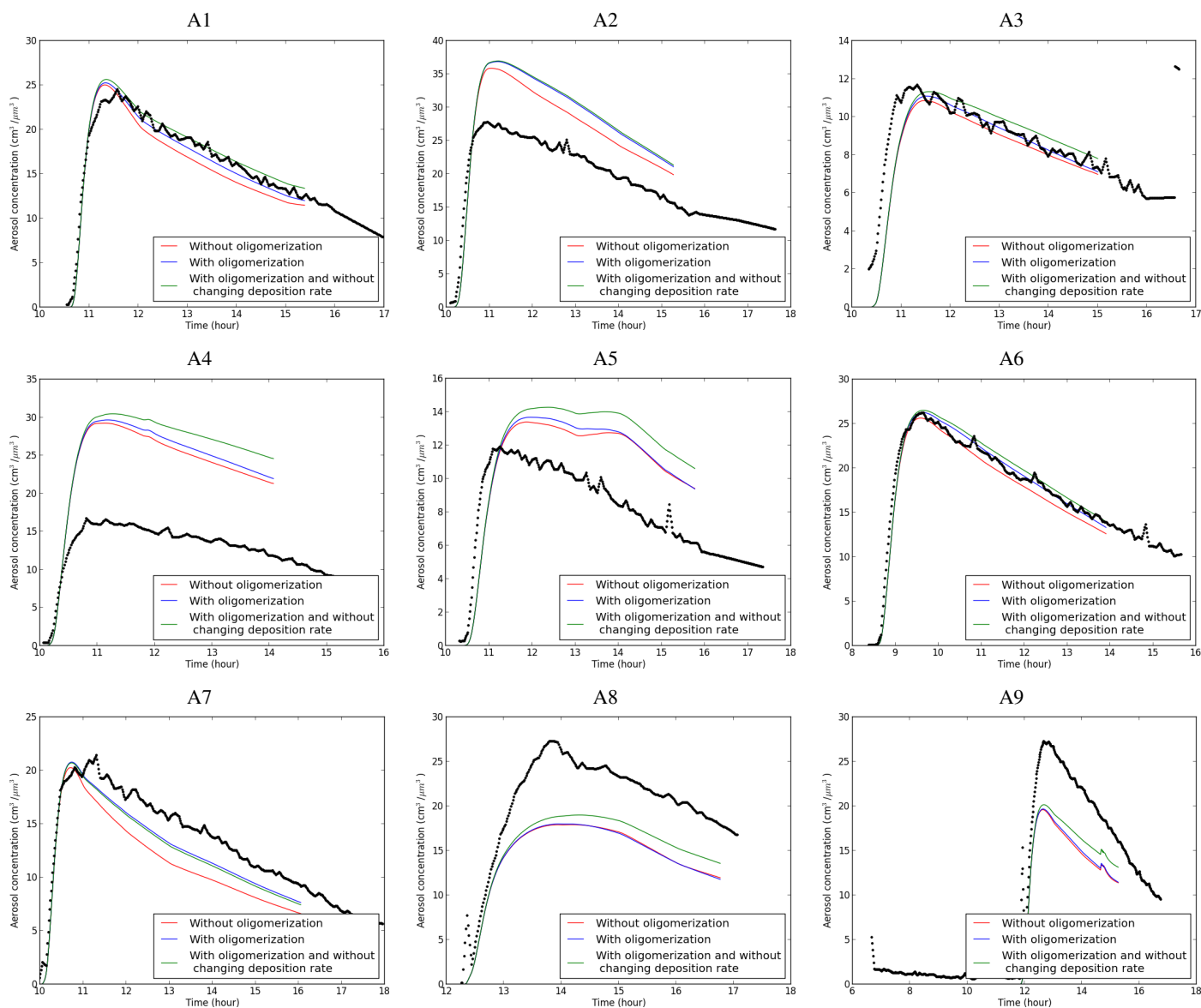


**Figure 5.** Aerosol concentration formation for the anthropogenic experiments. Black lines correspond to SMPS measurements.

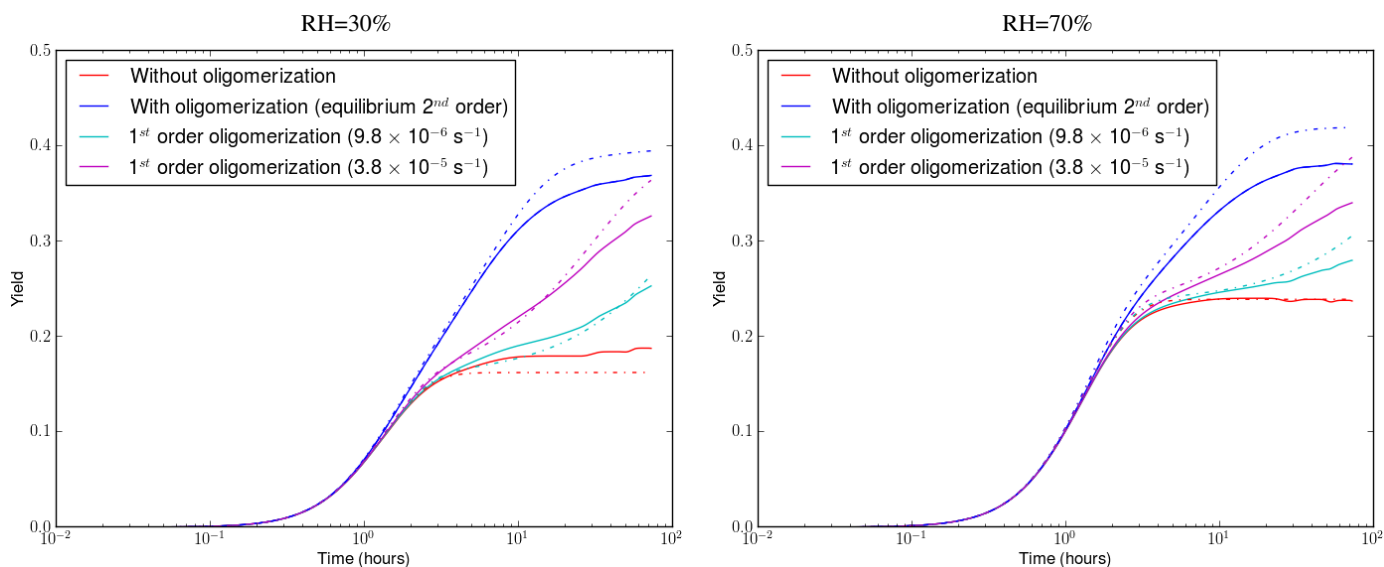


**Figure 6.** Evolution of the SOA yield from  $\alpha$ -pinene oxidation as a function of time for an organic mass loading of  $5 \mu\text{g m}^{-3}$ . Solid lines correspond to SOA formation with aging. Dashed lines (-) correspond to SOA formation without aging.

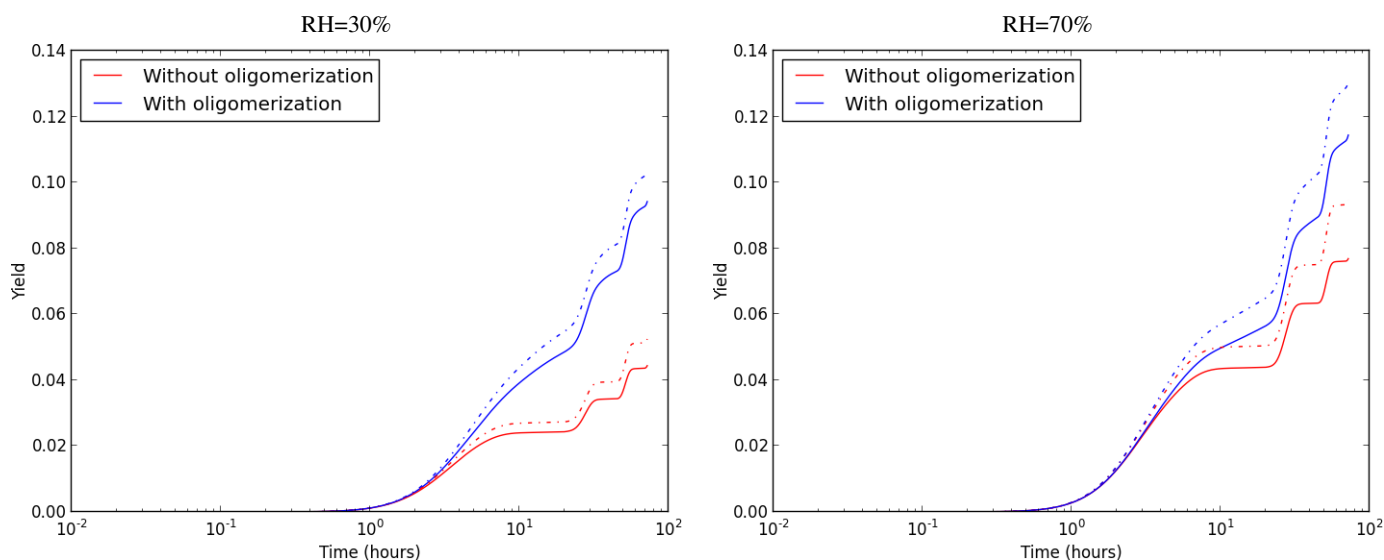


**Figure 7.** Evolution of the SOA yield from toluene oxidation as a function of time for an organic mass loading of  $5 \mu\text{g m}^{-3}$ . Solid lines correspond to SOA formation with aging. Dashed lines correspond to SOA formation without aging.

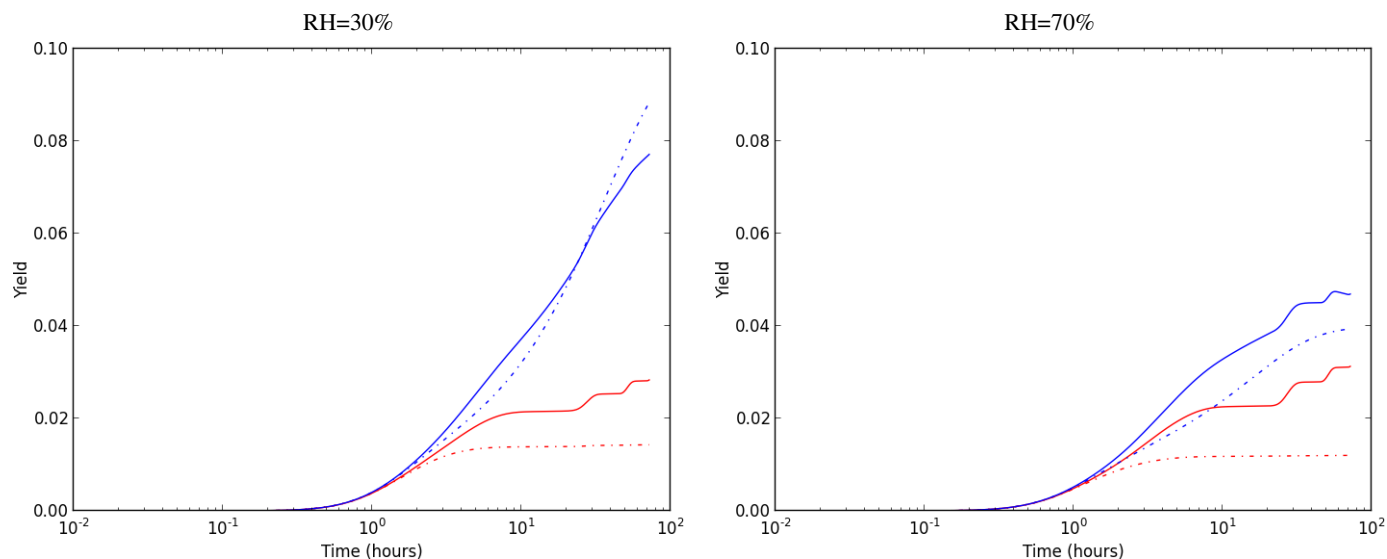


**Figure 8.** Evolution of the SOA yield from trimethylbenzene oxidation as a function of time for an organic mass loading of  $5 \mu\text{g m}^{-3}$ . Solid lines correspond to SOA formation with aging. Dashed lines correspond to SOA formation without aging.

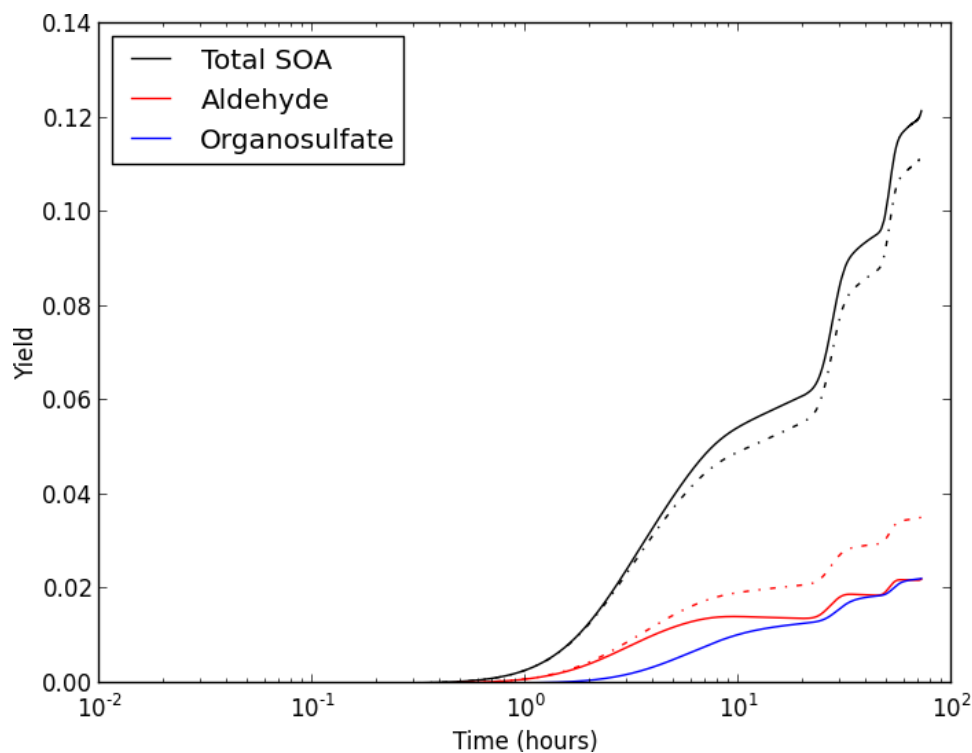


**Figure 9.** Yield of formation of SOA, aldehydes and organosulfates with (solid lines) or without (dashed lines) the conversion of aldehydes into organosulfates as a function of time for an organic mass loading of  $5 \mu\text{g m}^{-3}$  with  $2 \mu\text{g m}^{-3}$  of sulfates.



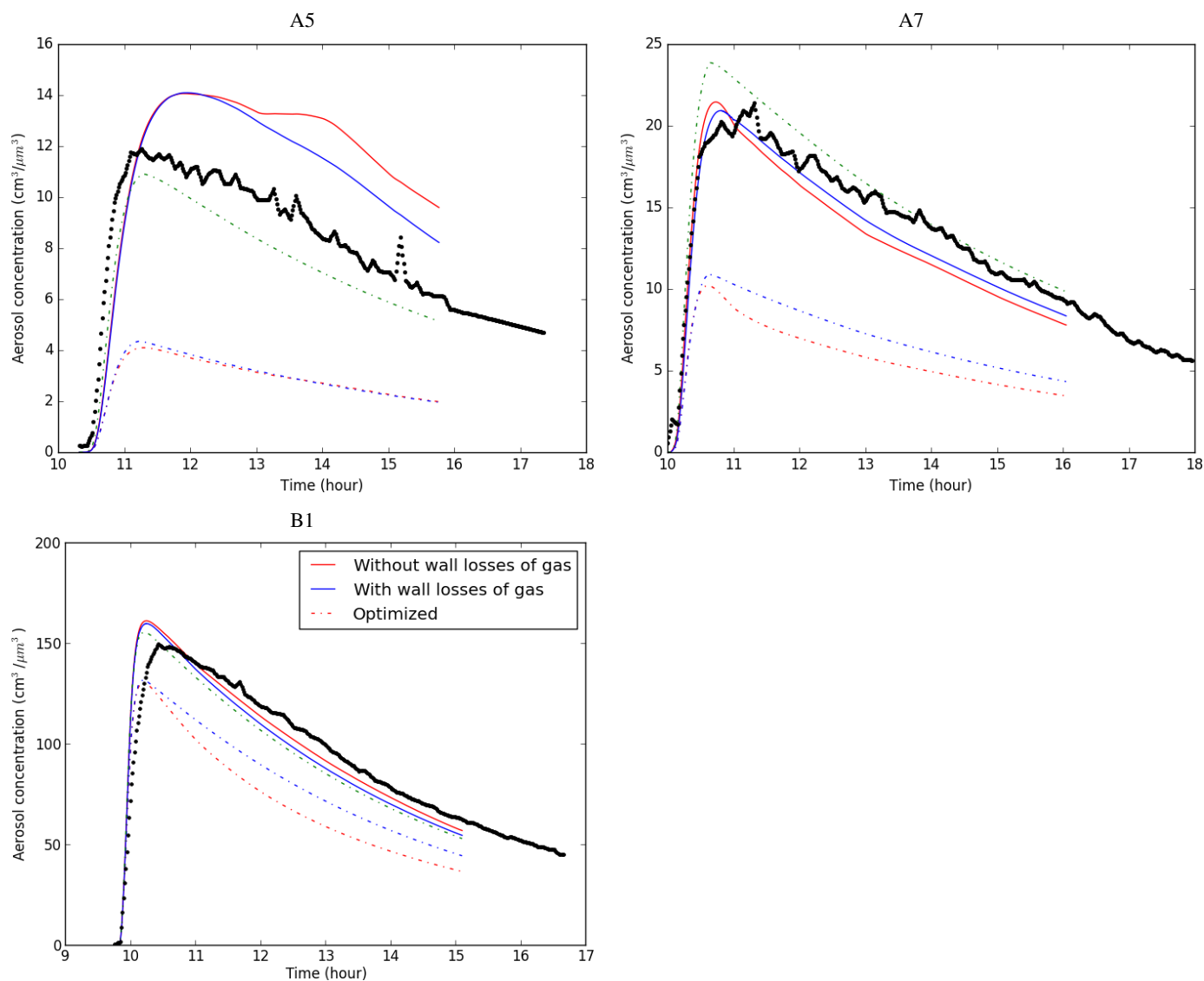


**Figure 10.** Effect of viscosity and gas wall losses on SOA concentrations for several experiments. The black line corresponds to SMPS measurements, the red lines correspond to modeled SOA concentrations for the non-viscous aerosol assumption, the blue lines correspond to modeled SOA concentrations for the viscous aerosol assumption, and the green lines correspond to modeled SOA concentrations for the viscous aerosol assumption with a decrease by a factor 3 of volatility. Solid lines correspond to simulations assuming no gas wall losses, dotted lines with gas wall losses.